

Microwave treatment of electric arc furnace dust with Tetrabromobisphenol A: Dielectric characterization and pyrolysis-leaching

Mohammad Al-harabsheh^{*1}, Sam Kingman², Ian Hamilton

¹ Chemical Engineering Department, Jordan University of Science and Technology, Irbid, 22110, Jordan

* msalharabsheh@just.edu.jo

²Faculty of Engineering, University of Nottingham, Nottingham, NG7-2RD, UK

Abstract

In the present work microwave treatment of electric arc furnace dust (EAFD) mixed with tetrabromobisphenol A (TBBPA) was investigated. A range of characterization techniques were used to understand the thermal behaviour of TBBPA-EAFD mixtures under microwave pyrolysis conditions. Dielectric and thermal properties of EAFD, TBBPA and their mixtures were determined. Both the dielectric constant and loss factor of the mixture were found to vary considerably with temperature and subsequently it was found that the mixtures of these materials absorbed microwaves effectively, especially at temperatures above 170°C. The high loss tangent of EAFD-TBBPA mixture above 170°C resulted in fast heating and high temperatures (above 700°C) resulting in reduction of Fe, Pb and Zn to their metallic form. This resulted in low recoveries of both Zn and Pb when the residue was leached in water. The recovery of Zn varied between 14 and 52 wt.%, while Pb recovery varied between 3 and 31 wt.% depending on microwave treatment efficiency. The low recovery of Zn and Pb could be ascribed by the reduction of metal oxides into their metallic form. More importantly this work has shown great selectivity in the leachability of both zinc and iron; with iron being left in the solid residue.

Keywords: EAFD; Dielectric Properties, Microwave treatment; Leaching; zinc extraction; TBBPA

1. Introduction

Electric Arc Furnace Dust (EAFD) is a waste by-product generated by the secondary steelmaking industry. Treatment of EAFD is of prime importance for environmental and resource conservation

27 as it is considered as an environmentally hazardous waste according to the Environmental
28 Protection Agency (EPA) as it contains easy leachable metals including Cd, Pb, and Cr [1, 2]. Due
29 to the depletion of the primary resources of metals such as Zn and Pb, recycling of this dust has
30 gained greater interest among researchers and investors in the metallurgical sector [3]. Both
31 Pyrometallurgical and hydrometallurgical methods have been suggested to recover valuable metals
32 from EAFD. Although pyrometallurgical treatment of EAFD is practiced now at the industrial
33 scale utilizing Waelz Kiln technology [4] and rotary hearth furnaces [5] to recover zinc in the form
34 of ZnO, these methods suffer from high energy requirements compared to hydrometallurgical
35 methods.

36 Different leaching reagents including sulphuric acid [6, 7], hydrochloric acid [8], ammonia [9, 10],
37 sodium hydroxide [11, 12], and some organic acids [13] have been used for extraction of zinc and
38 other valuables from EAFD. According to Jha et al [14], the most effective lixivants for zinc
39 extraction from EAFD were found to be sulphuric acid and ammoniacal solutions. Sodium
40 hydroxide, dissolves zinc selectively, however, this application needs further development for
41 effective metal recovery from the sodium zincate solution by electrolysis.

42 There is a great interest nowadays to utilize waste halogenated plastic materials for the recovery
43 of valuable materials from EAFD and to minimize its environmental impact as well as that of waste
44 plastics. Among these waste plastic materials are flame retardant materials, with
45 tetrabromobisphenol A (TBBPA) being the most widely used. Thermal treatment of these wastes
46 results in release of large amounts of HBr and other brominated organic substances such as
47 brominated phenols as well as wide array of other brominated organic compounds [15-19]. If
48 TBBPA is pyrolysed in the presence of metal oxides, the later has high fixing ability toward HBr
49 and subsequent reduction of brominated organic compounds released during the pyrolysis process
50 [15, 20].

51 The largest volume brominated flame retardant in production today is TBBPA [21]; its annual
52 production exceeded 170 kilotons in 2004 [22] and the estimated annual market demand from 2001
53 to 2003 was >200,000 ton/year [23]. The reports suggest that huge quantities of brominated plastic
54 wastes are accumulated worldwide, which makes their disposal a real and current challenge.

55 Utilization of EAFD as a debromination catalyst for TBBPA based plastic materials offers
56 numerous benefits such as HBr capture liberated during TBBPA pyrolytic incineration in the form

57 of metal bromides. These can be recovered in their vapor form or leached from the pyrolysis
58 residue using just water. Such a technique allows two waste materials to be treated concurrently
59 ~~con-currently~~ to minimize their associated risks and at the same time recover valuable metals from
60 EAFD by relatively simple means.

61 A major decomposition product from TBBPA degradation is HBr; which is an excellent
62 brominating agent for ZnO present in EAFD and, it therefore, can be used as an agent to selectively
63 separate zinc as a volatile bromide from the solid dust residues. These properties lead to the use of
64 TBBPA as a source of (HBr) for zinc recovery from EAFD as zinc bromide $ZnBr_2$ [24, 25].

65 The de-bromination process is mainly the loss of bromination species from the backbone followed
66 by an evaporation process. Hydrogen ~~bromide~~bromide (HBr) as the brominating agent is
67 generated in relatively large amounts when the TBBPA decomposes during thermal processing
68 (HBr accounts for ca. 59 wt.% of TBBP upon thermal decomposition). The HBr reacts with zinc
69 minerals forming a bromide ($ZnBr_2$) that has a boiling point of $650^{\circ}C$. Grabda et al [24] studied
70 the effect of heating time and temperature on the vaporizing of $ZnBr_2$ under different conditions.
71 They observed that the evaporation increases with heating time at constant heating rate and
72 increasing temperature (due to an increase in the vapor pressure). A mixture of argon and oxygen
73 were used to oxidize the high molecular weight compound ('char') that formed during thermal
74 decomposition of the TBBPA and this affected the vaporization process; however this complex
75 residue declined as heating time and temperature increased. The measured vaporization data show
76 that at $950^{\circ}C$ the vaporization of $ZnBr_2$ was complete, with less than 11 wt% char. However, one-
77 third of ZnO remained as un-reacted residue and required further treatment by carbothermic
78 reduction by carbonaceous char where 4 wt% remained in solid residue. Grabda et al. [26]
79 continued to investigate the possibility of EAFD treatment, using TBBPA and
80 tetrabromobisphenol A diglycidyl ether (TBBPADGE) at $550^{\circ}C$ for 80 min, under oxidizing and
81 inert atmospheres; a maximum of 85wt.% of zinc and 81wt.% of lead recoveries were achieved
82 using TBBPADGE. Oleszek-Kudlak et al. [27] also studied the reaction ~~of-between~~ TBBPA ~~with~~
83 and EAFD and the effect of temperature on the ~~process~~ of bromination zinc oxide and the
84 evaporation of ~~the metal oxides~~ its bromide ($ZnBr_2$) in the temperature range $250 - 950^{\circ}C$.

85 This work aims at evaluating the possibility of heating EAFD-TBBPA mixtures by microwave
86 irradiation under pyrolysis conditions. It also aims to study the possibility of extracting valuable

87 metals from the pyrolysis residue by a hybrid microwave pyrolysis-extraction method. Therefore,
88 the dielectric properties of both materials (EAFD and TBBPA) and their mixtures were measured
89 using cavity perturbation technique and reported herein. Additionally, the pyrolysis of EAFD-
90 TBBPA mixtures, under microwaves, followed by leaching of microwave pyrolysis residue were
91 also carried out.

92 **2. Experimental work**

93 **2.1. Materials**

94 The EAFD sample was collected from a Jordanian steel smelter. After homogenization by repeated
95 cone and quartering, the sample was characterized for its chemical and mineralogical composition.
96 A **Perkin Elmer (Optima® 3300 DV)** Inductively Coupled Plasma Atomic Emission Spectrometer
97 (ICP-AES), was used to measure the content of elements in the EAFD following the procedure of
98 sample preparation reported by Al-~~harahsheh~~-Harahsheh et al [28]. TBBPA was purchased from
99 Sigma Aldrich. All other chemicals were reagent grade and used without further purification.

100 **2.2. Microwave treatment procedure**

101 The description of the experimental setup used for microwave treatment of the EAFD-TBBPA
102 mixtures is reported elsewhere [29]. It consisted of a 3 kW microwave generator operated at 2.45
103 GHz a forward and reflected power measurement system connected to a PC, a WR340 standard
104 rectangular waveguide operating in a dominate TE_{10} mode coupled to a cylindrical choke section
105 (for sampling). The reaction system consisted of nitrogen cylinder fitted with a **flow_meter**, a
106 vertical quartz tube fitted inside the vertical applicator, two 250 ml gas wash bottles connected in
107 series and operated as gas extraction system, and vent connected to external extraction system.

108 EAFD was mixed with TBBPA in a tumbling mill with ceramic balls at a mass proportion of 1:1.
109 The mixture was then made into cylindrical pellets of about 5g mass. A hydraulic oil press was
110 then used to compress approximately 5 g of the mixture at 180 kg f/cm² for 60 s.

111 To perform the microwave pyrolysis experiments the pellets were placed in a quartz tube
112 positioned vertically in the cylindrical microwave applicator. The sample was then irradiated with

113 microwave energy for a specified time and power level while nitrogen gas purged the reaction
114 system. In order to collect any soluble vapors, the produced gases were vented through two gas
115 wash bottles filled with water. Irradiation time was varied depending on the observations of the
116 reaction systems and also based on the temperature reading obtained by an optical pyrometer.
117 Microwave power was shut-off if arcing occurred.

118 At the end of the experiment, the solid residues were reweighed and removed from the quartz tube.
119 Hot water was used to wash out the whole extraction system to collect any water soluble
120 condensate. It was then analyzed for metal content using ICP.

121 **2.3. Leaching of the microwave pyrolysis residues**

122 The solid residue after microwave treatment was ground to a particle size of less than 1 mm and
123 then subjected to leaching in boiling deionized water for 20 minutes. The mixture was then filtered
124 and the leaching solution was then analyzed for the metal content. The remaining solid residues
125 were also analyzed by X-ray diffraction (XRD) and Scanning Electron Microscopy (SEM).

126 **2.4. Measurement of dielectric properties**

127 Cavity perturbation method was employed to measure the dielectric properties of EAFD, TBBPA,
128 and their mixture. The experimental setup details are reported elsewhere [30]. A representative
129 mass of about 0.1-0.2 g of the material was packed in the quartz tube and heated to the desired
130 temperature, then positioned in the microwave resonant cavity by means of an automated actuator.
131 The frequency shift and quality factor were measured at 2470 and 912 MHz which are close to the
132 most frequently used frequencies in domestic and industrial microwave processes. Extra care was
133 taken to obtain similar packing density of samples, because powdered sample density has a great
134 effect on the measured values of dielectric properties [31]. The variation in density of packing for
135 3 replicates was determined to be less than 3.5%. Additionally for each sample, a minimum of
136 three replicates were measured. The dielectric constant (ϵ') and loss factor (ϵ'') were then calculated
137 [30].

138 **2.5.X-Ray diffraction and TGA analyses**

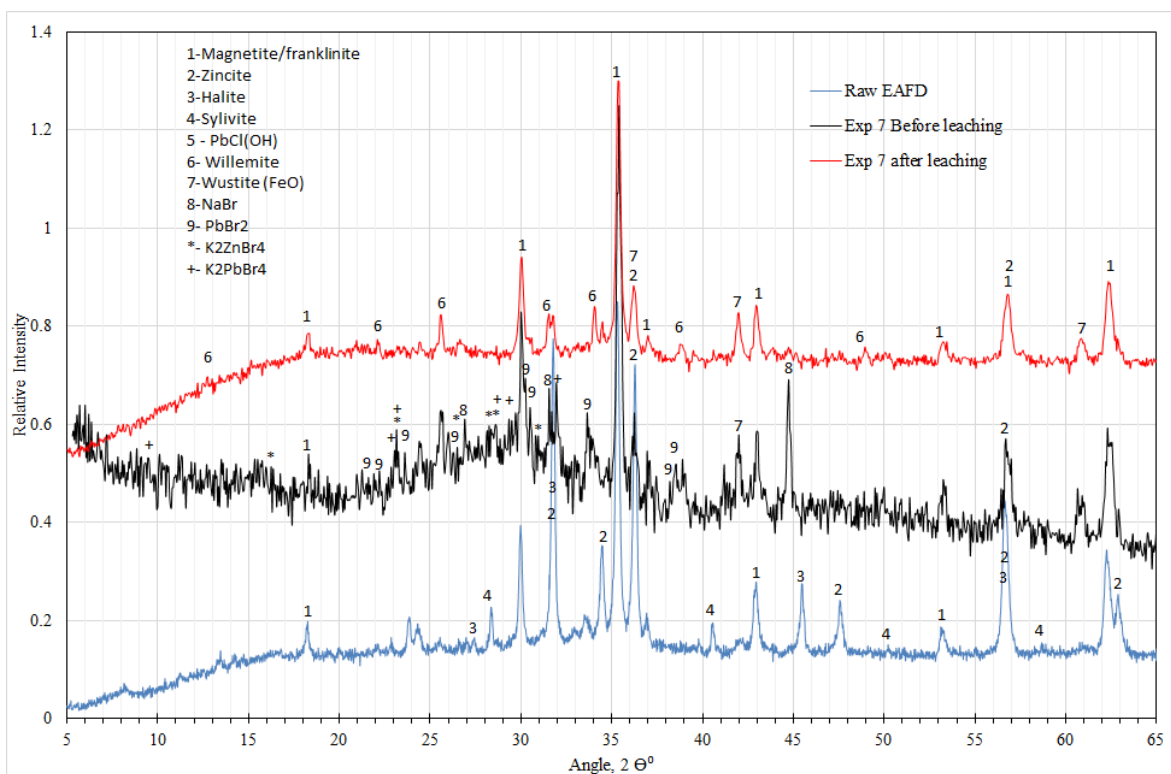
139 Representative EAFD sample, taken after prolonged manual mixing, was analyzed for its
140 mineral composition using X-ray diffraction analysis (XRD), furthermore, additional solid
141 samples were analyzed by XRD after microwave pyrolysis and after leaching experiments. A
142 Hiltonbrooks® generator with a Philips® PW 1050 diffractometer with an automatic divergence
143 slit, and Cu-K α anode producing X-rays of wavelength $\lambda= 1.54056 \text{ \AA}$ was used.

144 Thermogravimetric (TGA) and differential thermal analyses (DTA) of the dust (EAFD) and
145 the plastic material (TBBPA) and their mixture containing 50wt % EAFD and 50wt% TBBPA
146 were performed using a TA- Q600 thermal analyzer. About 10 mg of the sample was placed in
147 fused alumina pan and heated at a heating rate of 10°C/ min under nitrogen with a flow rate of 50
148 ml/min.

149 **3. Results and discussions**

150 **3.1.Physical and chemical characteristics of EAFD**

151 Figure 1 shows the XRD pattern of EAFD. The dust contains zincite, magnetite, franklinite,
152 halite, sylvite, lead hydroxyl chloride and hematite



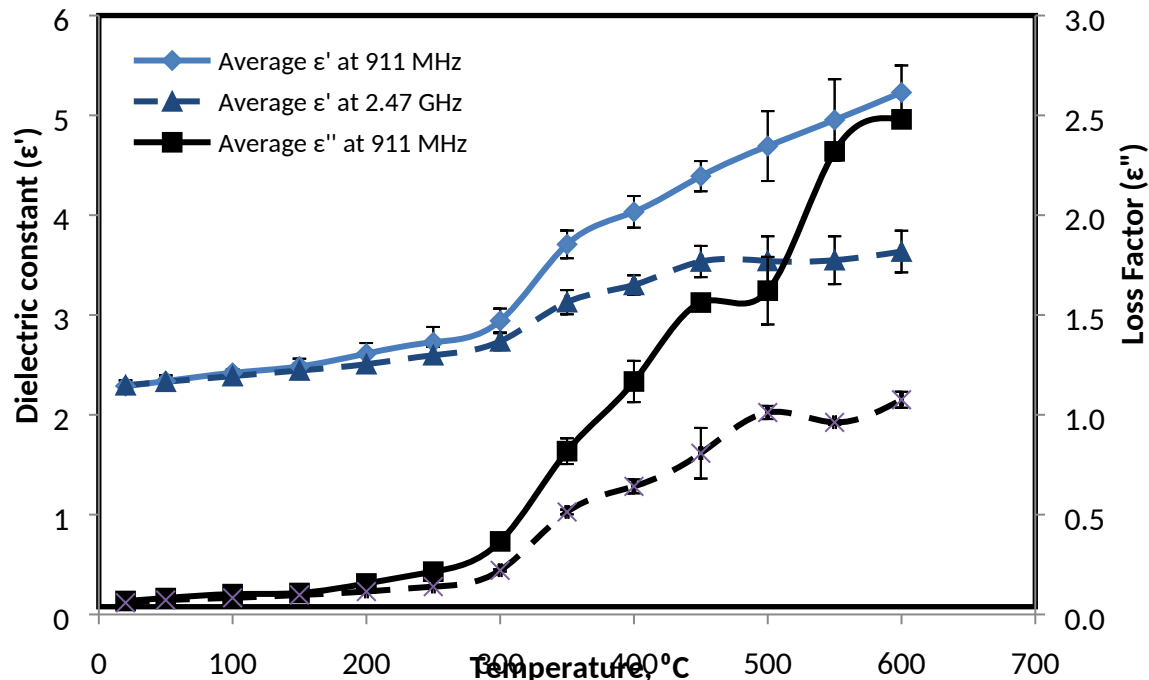
153

154 **Figure 1 XRD pattern for EAFD, EAFD-TBBPA residue after pyrolysis and after leaching**

155 The chemical composition of the EAFD sample used in this work was reported elsewhere
 156 [32]. The main elements present in the dust are: (in wt%) 25.9% Zn, 18% Fe, 4% Ca, 3.3% Na,
 157 3.2% Pb, 2.8% Si, 1.8% K and 1.2% Mn. Calorimetry showed that dust contains 2.63 ± 0.03 wt%
 158 total carbon and 0.1 wt% inorganic carbon suggesting that among mineral phases present in the
 159 dust are carbonates such as calcium carbonates.

160 **3.2. Dielectric properties of the EAFD**

161 The dielectric constant characterizes the capability of materials to absorb electromagnetic
 162 radiation, whereas, loss factor denote the ability of materials to dissipate the adsorbed radiation
 163 into heat. The dielectric constant and loss factor of EAFD were measured at two frequencies
 164 namely 911 MHz and 2.47 GHz across a temperature range from 25 to 600 °C [29]. Figure 2 shows
 165 the plot of dielectric constant (ϵ') and loss factor (ϵ'') as a function of temperature. Both values
 166 increase with an increase of temperature and the rate of increase become greater when the
 167 temperature exceeded 300 °C.



168

169 **Figure 2 Dielectric properties of EAFD as a function of temperature) at frequencies of 911MHz and 2.47 GHz [4].**

170 Additionally, the ratio of dielectric loss to the dielectric constant is called loss tangent ($\frac{\epsilon''}{\epsilon'}$).

171 When the loss tangent is above 0.05, the material is considered to heat well under microwave

172 irradiation. The loss tangent calculated for EAFD was found also to increase steadily with the

173 increase of temperature up to 300°C, then it increases considerably with a further increase of

174 temperature reaching a value of 0.3 at 600°C.

175 **3.3. Thermal and dielectric properties analysis of TBBPA**

176 **3.3.1. TGA of TBBPA**

177 Figure-3 shows the TGA profile for TBBPA at a heating rate of 10°C/min under nitrogen flushing

178 at a flowrate of 50mL/min. One major mass loss region is observed in the temperature region of

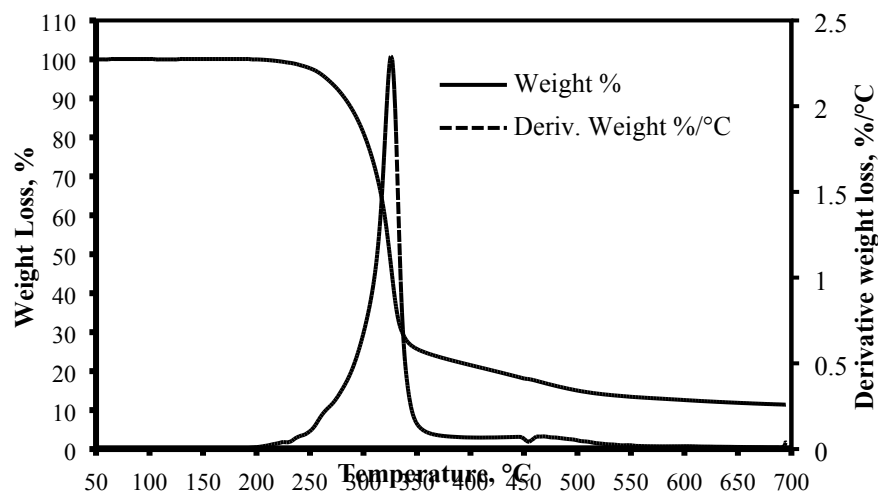
179 250-330°C, ascribed to the decomposition of TBBPA and the release of hydrogen bromide (HBr).

180 The mass loss in this region was around 75% of the initial mass. The theoretical content of HBr in

181 the TBBPA is 59.51%, which suggest that at least 15% of volatile hydrocarbons are evolved with

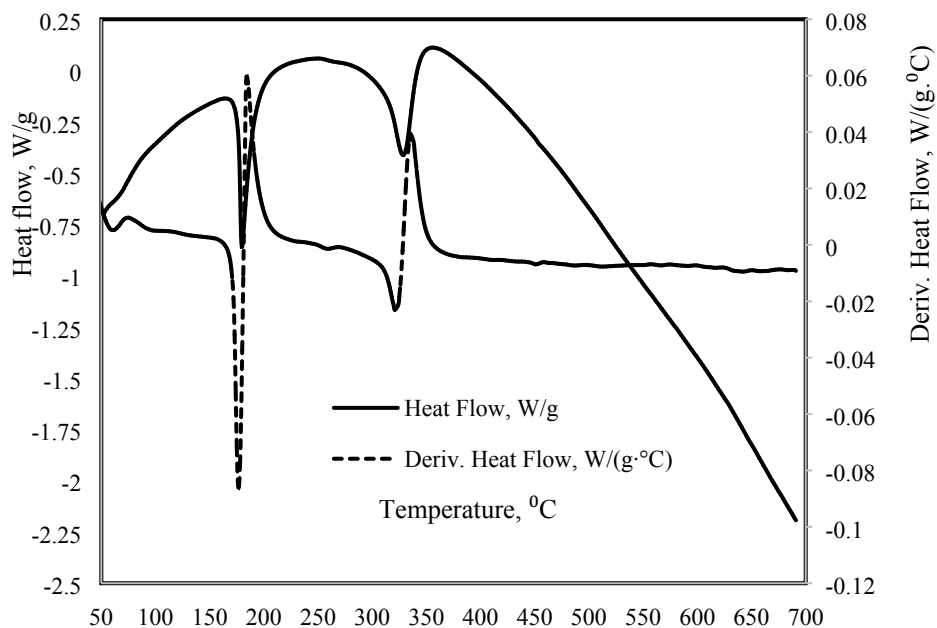
182 the HBr such as brominated phenols [15].

183 Figure 4 shows the DTA profile of the pure TBBPA. It exhibits two endothermic events. The first
184 event, occurring at a temperature of 178°C, indicated the smelting of TBBPA. The second event
185 occurring across a broad temperature region (250-350°C), with a maximum peak derivative heat
186 flow at 327°C, corresponds to TBBPA evaporation and decomposition and the evaporation of HBr
187 and organic hydrocarbons.



188

189 **Figure 3 TGA profile of TBBPA (heating rate=10C/min, N₂ flowrate=50mL/min**



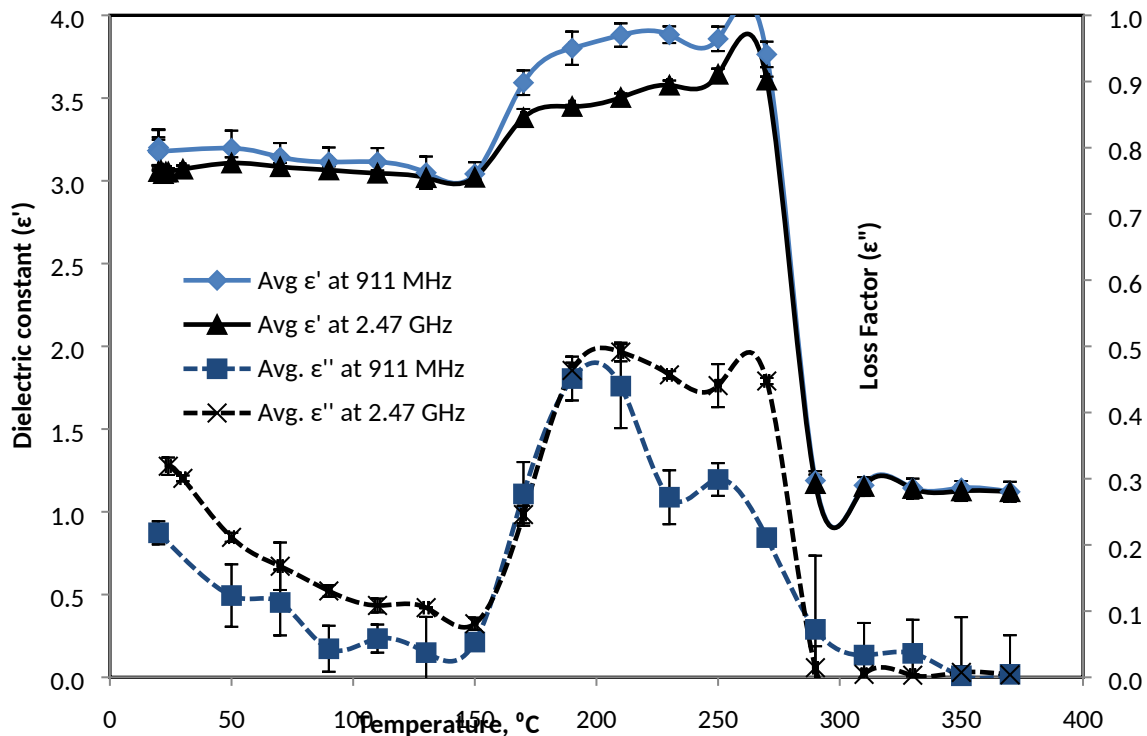
190

191 **Figure 4 DTA profile of TBBPA (heating rate=10C/min, N₂ flowrate=50mL/min**

192 ~~The thermal analysis of EAFD was reported by Al-Harashseh et al [29]. The main features of~~
193 ~~EAFD TGA profile include a mass loss appears at a temperature range of 160-200°C, assigned to~~
194 ~~the loss of associated moisture and possibly a level of bound water in metal chlorides present in~~
195 ~~the dust. A second mass loss was also observed in the temperature window 600-700 °C, assigned~~
196 ~~to the vaporization of metal chlorides, most likely ZnCl₂ [33]. The presence of ca. 2.6 % free~~
197 ~~carbon was thought to cause a reduction of some metal oxides such as ZnO to elemental zinc. The~~
198 ~~last mass loss region appearing at 770°C may be related to the energy intensive evaporation of~~
199 ~~zinc.~~

200 **3.3.2. Dielectric Properties of TBBPA**

201 ~~Figure 5~~Figure 3 shows the dielectric properties of TBBPA as a function of temperature at
202 frequencies of 911 and 2.47 GHz. The dielectric constant remains constant until a temperature of
203 150°C then increases suddenly at a temperature of 170°C followed by steady increase until a
204 temperature of 270°C and then decreases sharply. The loss factor decreases with the increase in
205 temperature up to a temperature of 150°C then increases sharply up to a temperature of 270°C and
206 then drops sharply. The increase of both dielectric constant and loss factor after 170°C is related
207 to the start of smelting of TBBPA (melting point of TBBPA=178°C). However the sharp decrease
208 in both parameters after 270°C is an artifact related to the sharp reduction of sample volume due
209 to the decomposition of TBBPA. To obtain more accurate dielectric properties values, a volume
210 correction factor should be introduced; the weight loss at the decomposition temperature was
211 measured to be around 75 wt% of the initial mass. The data reported in Figure 5 did not take into
212 account the volume correction factor due to the difficulty in measuring the final volume at each
213 temperature.



214

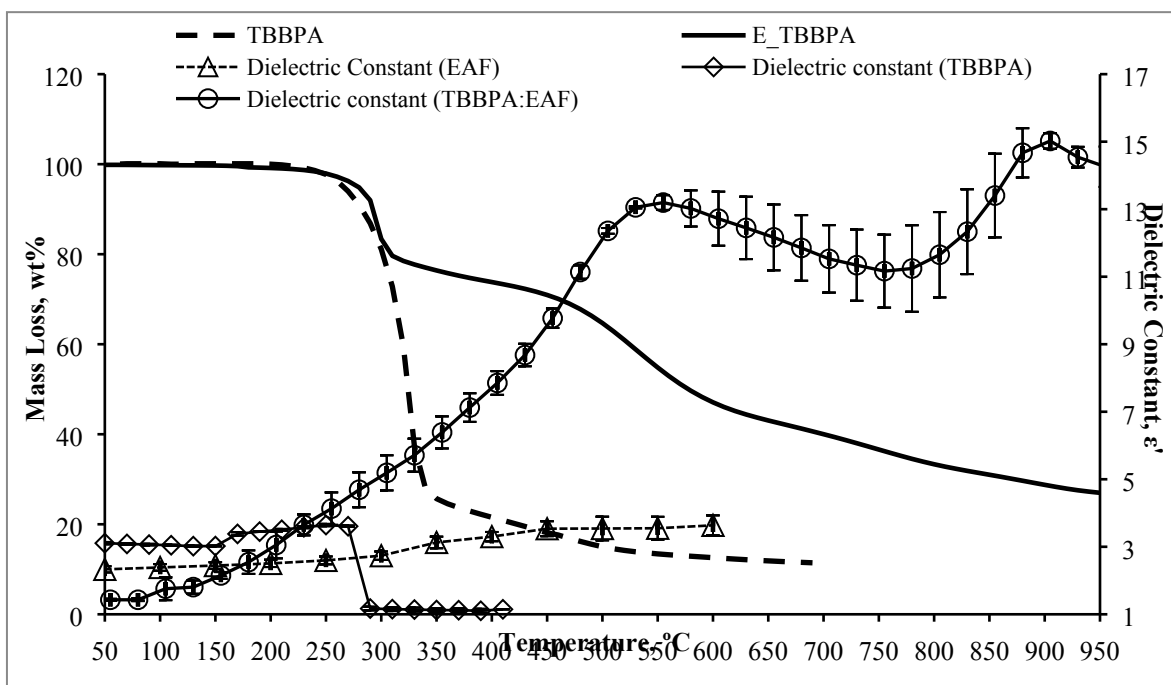
215 **Figure 3 Dielectric Properties of TBBPA as a function of temperature at frequencies of 911 MHz and 2.47 GHz**

216 **3.4. Thermal and dielectric properties of TBBPA-EAFD mixture**

217 To study the interaction of the TBBPA-EAFD mixture with microwaves it is essential to measure
 218 both dielectric constant and loss factor of the mixture. During thermal treatment of TBBPA-EAFD
 219 mixture several events are expected to occur, which will influence the dielectric properties of the
 220 mixture. Therefore, the change in mass loss, the heat flow, the dielectric constant and loss factor
 221 were measured at different temperatures for a mixture containing 50 wt. % TBBPA and 50 wt. %
 222 EAFD. The results of these measurements are plotted in [Figure 6 and Figure 7](#) [Figure 4 and Figure](#)
 223 [5](#).

224 The presence of EAFD with TBBPA altered the TGA decomposition profile of TBBPA. Two main
 225 regions of mass loss can be seen in the TGA profile for the TBBPA-EAFD mixture, whereas, only
 226 one mass loss was seen for pure TBBPA. The later corresponds to the decomposition of TBBPA
 227 which ended at a temperature of 350°C; the corresponding mass loss was 75wt% of the initial
 228 mass; the mass loss from EAFD alone at this temperature is only 2.5wt%. However, the mass loss
 229 for TBBPA-EAFD at the first decomposition stage, ending at a temperature of 310°C, and was

230 21.5wt% although the decomposition event occurred at the same initial temperature. With the
 231 mixture containing 50wt% TBBPA and the remainder consisting of EAFD; the expected mass loss
 232 based on the losses of pure materials was determined to be 38.75wt% [29, 34]. The 17.25wt%
 233 increase in residual mass found from the experiment is believed to be due to the HBr released not
 234 leaving the sample, instead being fixed in the dust in the form of metal bromide ($ZnBr_2$, $PbBr_2$,
 235 $CdBr_2$, $FeBr_2$, $FeBr_3$, etc). The exothermic event seen in the heat flow of the TBBPA-EAFD
 236 mixture at a temperature of 310°C was evidence of the formation of metal bromides as seen in
 237 ~~Figure 7~~Figure 5, whereas, an endothermic event was seen in the case of the pure TBBPA as a
 238 result of decomposition.



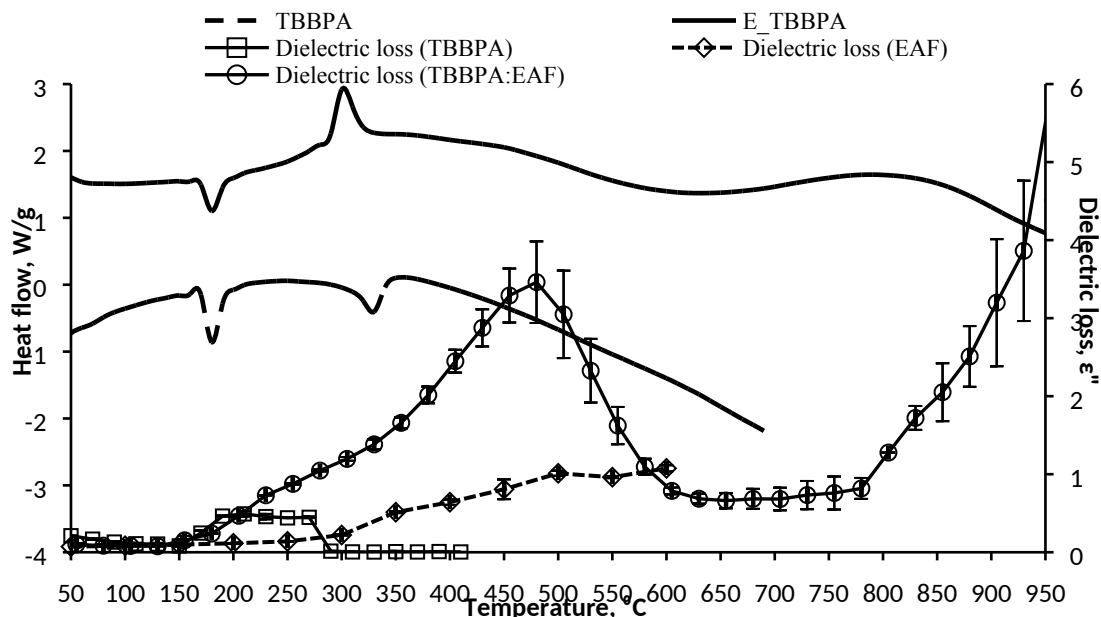
239
 240 **Figure 4 overlay of mass loss and dielectric constant measurement (2.47 GHz) of 1:1 mass ratio of TBBPA-EAFD mixture**
 241 **designated as E-TBBPA.**

242 The second decomposition stage (470-600°C) seen in the TG profile of TBBPA-EAFD mixture
 243 could be related to evaporation of zinc bromide formed [35]. Further mass loss occurring above
 244 temperature 600°C could be related to evaporation of other metal bromides species like $PbBr_2$ and
 245 $FeBr_2$ as well as reduction of the remaining metal oxides present in the dust by the char/carbon
 246 (evidence of this will be demonstrated later) and also evaporation of metallic zinc produced by
 247 reduction reactions.

248 The dielectric constant of the mixture did not correlate with the mass loss occurring at the first
249 decomposition stage as it increases with the increase in temperature up to a temperature of 550°C
250 reaching the first maxima of 13.2. The different behavior of dielectric constant of TBBPA-EAFD
251 mixture from that of pure TBBPA could be related to the formation ionic metal bromides which
252 coincide with TBBPA decomposition and the release of HBr. These halide ionic species exhibit
253 strong interaction with the electric field [29] due to ionic conduction and also the fusion of these
254 halides ($T_m(\text{ZnBr}_2)=394^\circ\text{C}$ [36]; $T_m(\text{PbBr}_2)=371^\circ\text{C}$) [37].

255 The steady drop in dielectric constant of the TBBPA-EAFD mixture beyond a temperature of
256 550°C until 760°C, reaching a minima of 11.16, could be related to the vaporization of the metal
257 bromides which corresponds to the second thermal event described above. Beyond a temperature
258 of 760°C, the dielectric constant starts to increase again reaching a second maxima (of 15.02) at a
259 temperature of 905°C. In this temperature region reduction of the remaining metal oxides occurs
260 by the char forming pure metal like Zn, Pb and Fe, as confirmed by SEM analysis shown below.
261 Furthermore, zinc boils at a temperature of 907 °C [36].

262 The loss factor of TBBPA-EAFD mixtures, remained at very low values until the TBBPA smelts
263 thereafter the values began to increase at a constant rate up to the decomposition temperature of
264 TBBPA. Further increases occurred with a higher rate until reaching a maximum value (3.46) at a
265 temperature of 480 °C-, which corresponds to the onset temperature of the second thermal event
266 (zinc bromide vaporization). The loss factor then dropped to values as low as 0.68 at a temperature
267 of 630°C then remained almost constant until the temperature reached 780 °C, where it was seen
268 to increase rapidly. The loss of the ionic metal bromides beyond a temperature of 480 °C appeared
269 to have contributed to the drop in the loss factor, however, the formation of the char at pyrolysis
270 temperature is likely to the cause of the sharp increase of the loss factor.



271
 272 **Figure 5** overlay of heat flow and dielectric constant measurement (2.47 GHz) of 1:1 mass ratio of TBBPA-EAFD mixture

273 3.5.Recovery of valuable metals

274 The recovery of valuable metals was performed for a TBBPA-EAFD mixture of mass ratio 1:1.
 275 This was performed in two stages; metals evaporated during microwave pyrolysis and metals
 276 leached from the pyrolysis residue using boiling water

277 The recovered metals from EAFD-TBBPA pellets after microwave pyrolysis in the extraction
 278 system is shown in Table 1. The same experiment was repeated 6 times due to the great variations
 279 in microwave coupling with the sample. Approximately 5wt% of zinc, 4wt% of lead and 6wt% of
 280 cadmium were collected as metal bromide vapor. Other distinctive features observed (shown in
 281 Table 1) was the absence of iron in the solution, implying that iron bromides were not evaporated
 282 from the pellet.

283 **Table 1** Valuable metals (wt%) recovered as condensate in the extraction system after microwave treatment.

Exp. #	Ca	Cd	Fe	K	Mg	Mn	Na	Pb	S	Zn
MH1	0.17	1.99	0.03	0.54	0.10	0.13	0.62	0.63	0.44	1.31
MH2	0.19	2.83	0.00	0.31	0.07	0.07	0.49	1.10	0.60	3.75
MH3	0.24	2.43	0.03	0.32	0.29	0.07	0.37	1.03	0.62	2.37
MH7	0.51	5.88	0.06	0.86	0.54	0.18	0.95	4.14	0.93	4.74
MH8	0.26	2.24	0.03	0.74	0.20	0.14	0.74	1.58	0.49	2.01
MH9	0.24	0.73	0.02	0.24	0.27	0.07	0.28	0.67	0.66	0.83

284 Table 2 shows the metal recovery from the TBBPA- dust mixtures after leaching of residues
 285 obtained in hot water for 20 minutes. Both K and Na show high recovery in the leaching solution,
 286 which is expected, as both K and Na are, initially, in the chloride form in the dust which are soluble
 287 in water. Cadmium recovery was as high as 87wt% in the leaching solution, while the highest lead
 288 and zinc recoveries were only 33wt% and 50wt%, respectively. These values were slightly lower
 289 than those obtained after conventional pyrolysis followed by leaching of the solid residues of E-
 290 TBBPA1 (1 Dust: 1 TBBPA) [12]. With regards to iron, no more 1wt% was recovered in the
 291 leaching solution and the remaining was mainly in the solid residue. This finding is of prime
 292 importance, which suggests that excellent selectivity of dissolution of lead and zinc with respect
 293 to iron, making further treatment of pregnant solution much simpler. Similar selectivity results
 294 were obtained under conventional pyrolysis conditions [34]. Additionally, both calcium and
 295 manganese showed good fixing capacity toward HBr.

296 **Table 2 Valuable metals (wt%) recovered from TBBPA-EAFD mixtures by leaching of the pyrolysis residues in boiling**
 297 **water for 20 minutes**

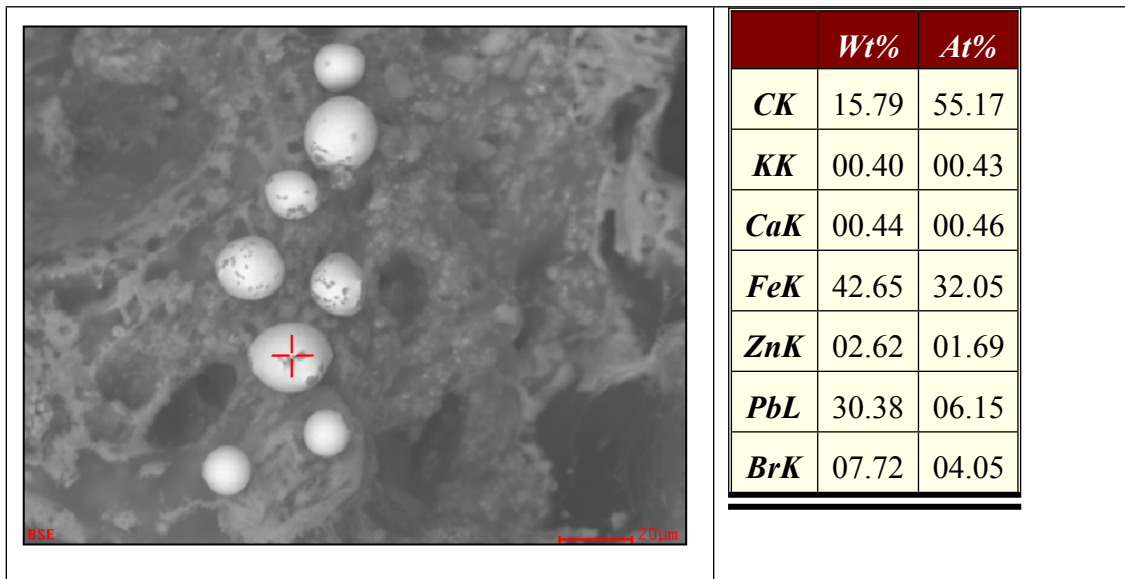
Exp. #	Ca	Cd	Fe	K	Mg	Mn	Na	Pb	S	Zn
ML1	29.83	67.52	0.00	76.69	12.13	7.93	74.21	3.14	17.05	12.63
ML2	46.19	58.80	0.00	87.09	7.01	23.55	86.72	7.58	8.71	27.36
ML3	49.04	79.45	1.30	93.87	8.41	28.98	92.36	20.48	17.82	46.69
ML7	50.74	80.66	0.47	97.15	4.14	33.10	95.72	31.00	16.59	45.57
ML8	52.48	81.74	0.08	95.24	5.60	30.64	93.35	24.16	32.67	50.38
ML9	48.32	87.13	0.19	96.92	3.67	34.26	95.05	14.92	10.98	42.04

298 For a better understanding of the reaction occurring between metal oxides present in the dust and
 299 the decomposition products of TBBPA (HBr and char), both SEM and XRD analyses of both
 300 pyrolysis and leaching residues were performed.

301 The XRD patterns of solid residues after microwave pyrolysis, and after leaching with hot water
 302 are shown in Figure 1. Table 3 shows the main mineral phases identified in the samples (EAFD,
 303 pyrolysis and leaching residue). After pyrolysis the peaks of zincite decreased considerably,
 304 however, still present in the sample after pyrolysis and leaching which explains the low zinc
 305 recovery which is also related to the presence of franklinite. This could be due to several reasons
 306 the principal one being that the HBr released from the TBBPA was
 307 stoichiometrically stoichiometrically not sufficient to convert all of ZnO and ZnFe₂O₄ to zinc
 308 bromide. It is worth mentioning that part of HBr was reacted with NaCl and KCl to form both
 309 NaBr and KBr.

310 The presence of chloride salts also led to the formation of complex salts such as Na_2ZnBr_4 ,
 311 Na_2PbBr_4 , K_2ZnBr_4 and K_2PbBr_4 . Additionally, the presence of wustite in the pyrolysis residue is
 312 an evidence of the partial iron oxide (magnetite) reduction.

313 SEM analysis of samples of the TBBPA-dust mixture after microwave treatment showed the
 314 formation of lead-iron nodules as can be seen from ~~Figure 8~~Figure 6. These lead-iron nodules were
 315 not observed after conventional pyrolysis of the same mixture even at temperatures as high as 450
 316 °C [34]. This suggests that the treatment temperature was high enough to carbonize the TBBPA
 317 and produce carbon that was able to reduce both iron and lead present in the dust. Such findings
 318 explain the lower recovery levels of iron, lead and zinc.



319 **Figure 6 SEM micrograph and EDX analysis of TBBPA-dust residue (1:1) after microwave treatment showing iron nodules**
 320 **coated with lead.**

321 The XRD pattern for residue after leaching showed also the presence of Pb(OH)Br in the solid
 322 residue, which explains the lower lead recovery than that of Zn. Ioannidis et al [38] reported that
 323 Pb(OH)Br can be precipitated in neutral water in the pH range between 4-8. This was confirmed
 324 by SEM and EDS analyses shown in ~~Figure 9~~Figure 7; the atomic ratio of Br and Pb is almost 1
 325 suggesting that the analyzed spot is Pb(OH)Br . The presence of Pb(OH)Br was also detected in
 326 the conventional pyrolysis residue of the same mixture (50wt% EAFD+ 50wt% TBBPA) after
 327 leaching [34]. Additionally, the atomic ratio of Fe, Zn and O is consistent with the presence of an
 328 Fe-Zn alloy and iron and/or iron-zinc oxides; the atomic ratio of elements in franklinite is
 329 $1\text{Zn}:2\text{Fe}:4\text{O}$, whereas, the ratio obtained in the area is $15\text{Zn}:19\text{Fe}:8\text{O}$ suggesting that almost

330 80wt% of Zn and Fe are in the form of Fe-Zn alloy. The latter was confirmed by XRD analysis
 331 (see Table 3). However, such alloy was not detected in the previous work by Al-Harashseh et al
 332 [34] following conventional pyrolysis, which again confirms the high temperatures obtained by
 333 microwave heating. The formation of char coupled with the high temperatures led to reduction of
 334 Fe and Zn oxides into their metallic forms, while arcing during microwave pyrolysis have to their
 335 smelting and formation of such Fe-Zn alloys.

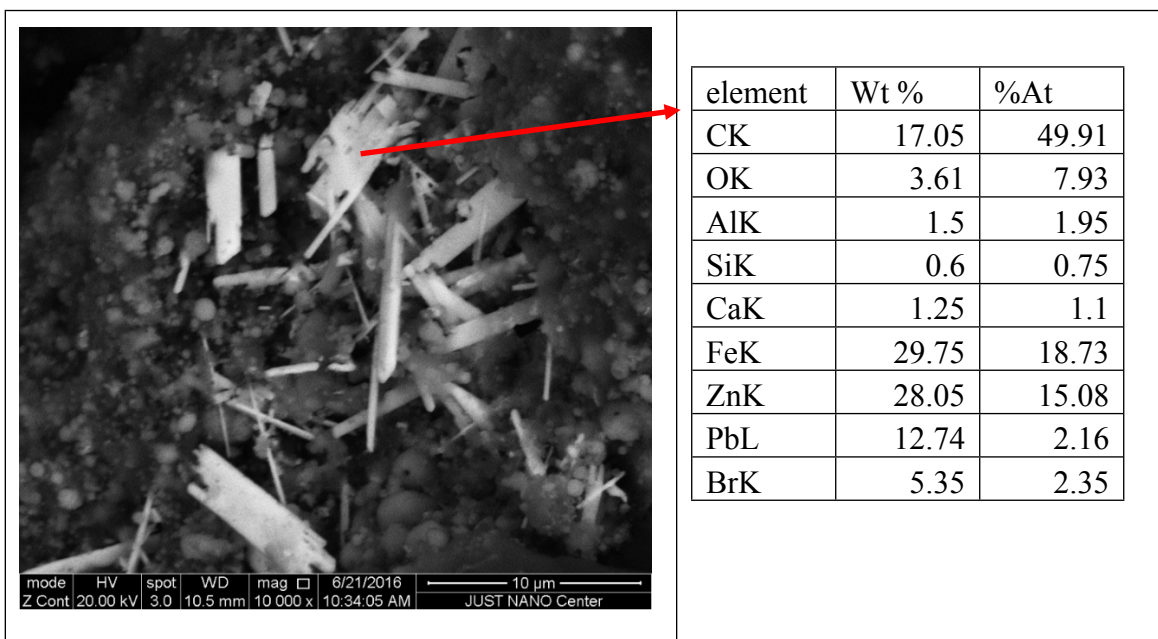
336 In summary, it was found that microwave heating was efficient for the pyrolysis of TBBPA-EAFD
 337 mixture in very short time (less than 2 minutes). An example of the power profile obtained during
 338 microwave treatment of the mixture is shown in Figure 8. The amount of microwave power
 339 absorbed increased rapidly reaching almost 80% of the incident power, and then dropped to almost
 340 30%, followed by further increased to 60% after 1 minute then it remained -constant. The absorbed
 341 power profile is consistent with the variations in both dielectric constant and loss factor observed
 342 shown in Figure 4 and Figure 5. (less than 2 minutes). After 115 seconds of microwave arcing was
 343 observed, therefore, the microwave power was shutoff. The maximum temperature detected by the
 344 optical pyrometer was about 650 °C. However, for the purpose to recover metal values by leaching
 345 of pyrolysis residue, it is required that the microwave pyrolysis temperature should not exceed
 346 350°C to avoid evaporation of metal bromides and the reduction of these metals into their metallic
 347 form. Additionally, the ratio of TBBPA to EAFD should be increased to offer more HBr to convert
 348 both zinc and lead oxides into soluble metal bromides. The recent work by Al-Harashseh et al [34]
 349 have shown that conventional pyrolysis TBBPA-EAFD mixture up to a temperature of 350°C
 350 followed by leaching of pyrolysis residue results in very high recoveries of both Zn and Pb leaving
 351 Fe in the pyrolysis residue.

352
 353 **Table 3 Mineral phases identified in the residue of EAFD-TBBPA (1:1) after microwave treatment and after water leaching.**

Feed EAFD	Franklinite/Magnetite, Zincite, Halite, Sylvite, PbCl(OH), calcite, silicate
EAFD-TBBPA residue after microwave pyrolysis	Franklinite/Magnetite, Zincite, PbBr ₂ , Willemite, Wustite, NaBr, KBr, K ₂ ZnBr ₄ , K ₂ PbBr ₄ , Na ₂ ZnBr ₄ , Na ₂ PbBr ₄ , Iron, Lead, Iron-zinc

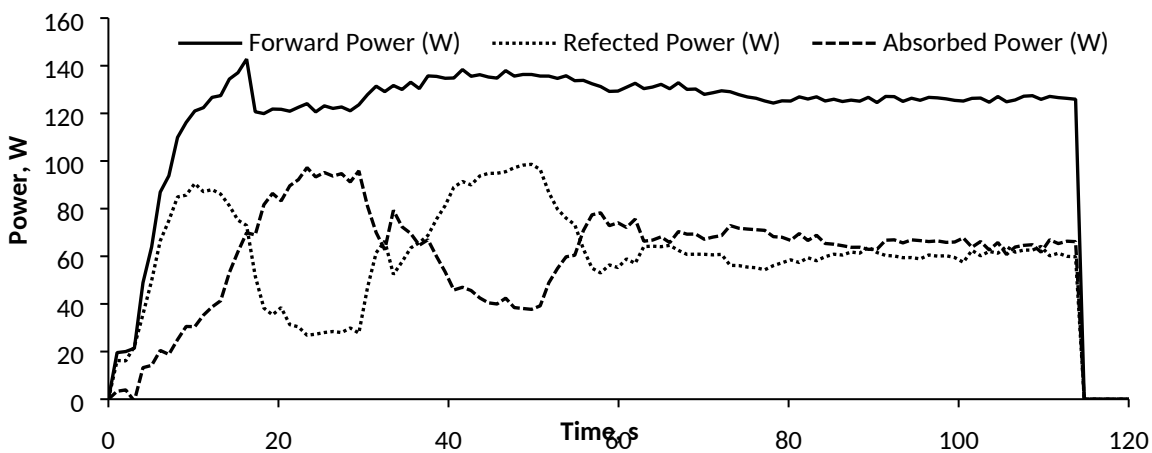
EAFD-TBBPA residue after microwave pyrolysis and leaching	Franklinite/Magnetite, Zincite, Willemite, Wustite, Hematite, Iron, Lead, iron-zinc, PbBr(OH)
---	---

354



355 **Figure 7 SEM micrograph and EDX analysis of TBBPA-dust residue (1:1) after microwave treatment and leaching showing PbBrOH precipitate**

356



357

358 **Figure 8 Example of microwave power log obtained for Exp. MH 3**

359

360 4. Conclusions

361 Comprehensive characterization of EAFD-TBBPA mixture (ratio 1:1) was carried out in terms of
362 their dielectric and thermal behavior as well as chemical and mineralogical composition. The
363 TBBPA-EAFD mixture exhibited good absorption of microwaves once the melting temperature
364 of the TBBPA has been reached. The microwave treatment time was short (1-3 minutes)
365 suggesting the high efficiency of microwave treatment. Microwave treatment of EAFD-TBBPA
366 mixture followed by water leaching was found to be not very efficient for recovery of Zn, and Pb
367 due to the reduction of these metals into their metallic form by the carbonaceous materials left
368 after TBBPA decomposition and also due to the low proportion TBBPA used in the mixture. The
369 SEM and XRD analyses confirmed that part of iron, lead and zinc oxides present in the dust were
370 reduced to their metallic form. Additionally Pb was found to precipitate during the leaching
371 process in the form of PbBrOH which implies that Zn and Pb can be separated during leaching of
372 the residue.

373 The pyrolysis of TBBPA in presence of EAFD is showed to be good method of debromination of
374 TBBPA to form a high value product. Although further work will be required to evaluate the
375 possibility of the emission of hazardous brominated organic compounds

376 5. References

- 377 [1] T. Suetens, B. Klaasen, K. Van Acker, B. Blanpain, Comparison of electric arc furnace dust
378 treatment technologies using exergy efficiency, *Journal of Cleaner Production*, 65 (2014) 152-167.
- 379 [2] EAP, European Waste Catalogue And Hazardous Waste List in, Environmental Protection
380 Agency, 2002.
- 381 [3] E. Abkhoshk, E. Jorjani, M.S. Al-Harashseh, F. Rashchi, M. Naazeri, Review of the
382 hydrometallurgical processing of non-sulfide zinc ores, *Hydrometallurgy*, 149 (2014) 153-167.
- 383 [4] J. Rütten, C. Frias, G. Diaz, D. Martin, F. Sanchez, Processing EAF dust through Waelz Kiln
384 and ZINCEXTM solvent extraction: the optimum solution, in: *European Metallurgical*
385 *Conference, SME, Düsseldorf/ Germany, 2011, pp. 1673-1688.*
- 386 [5] H. Oda, T. Ibaraki, Y. Abe, Dust recycling system by the rotary hearth furnace, in: *Nippon*
387 *Steel Technical Report, 2006, pp. 147-152.*
- 388 [6] T. Havlik, M. Turzakova, S. Stopic, B. Friedrich, Atmospheric leaching of EAF dust with
389 diluted sulphuric acid, *Hydrometallurgy*, 77 (2005) 41-50.

- 390 [7] F. Kukurugya, T. Vindt, T. Havlík, Behavior of zinc, iron and calcium from electric arc furnace
391 (EAF) dust in hydrometallurgical processing in sulfuric acid solutions: Thermodynamic and
392 kinetic aspects, *Hydrometallurgy*, 154 (2015) 20-32.
- 393 [8] D.S. Baik, D.J. Fray, Recovery of zinc from electric-arc furnace dust by leaching with aqueous
394 hydrochloric acid, plating of zinc and regeneration of electrolyte, *Mineral Processing and*
395 *Extractive Metallurgy*, 109 (2000) 121-128.
- 396 [9] Z. Youcai, R. Stanforth, Integrated hydrometallurgical process for production of zinc from
397 electric arc furnace dust in alkaline medium, *J. Hazard. Mater.*, 80 (2000) 223-240.
- 398 [10] K. Gargul, B. Boryczko, Removal of zinc from dusts and sludges from basic oxygen furnaces
399 in the process of ammoniacal leaching, *Archives of Civil and Mechanical Engineering*, 15 (2015)
400 179-187.
- 401 [11] A.J.B. Dutra, P.R.P. Paiva, L.M. Tavares, Alkaline leaching of zinc from electric arc furnace
402 steel dust, *Miner Eng*, 19 (2006) 478-485.
- 403 [12] C. Jarupisitthorn, T. Pimtong, G. Lothongkum, Investigation of kinetics of zinc leaching from
404 electric arc furnace dust by sodium hydroxide, *Materials Chemistry and Physics*, 77 (2003) 531-
405 535.
- 406 [13] J.M. Steer, A.J. Griffiths, Investigation of carboxylic acids and non-aqueous solvents for the
407 selective leaching of zinc from blast furnace dust slurry, *Hydrometallurgy*, 140 (2013) 34-41.
- 408 [14] M.K. Jha, V. Kumar, R.J. Singh, Review of hydrometallurgical recovery of zinc from
409 industrial wastes, *Resources, Conservation and Recycling*, 33 (2001) 1-22.
- 410 [15] O. Terakado, R. Ohhashi, M. Hirasawa, Thermal degradation study of tetrabromobisphenol
411 A under the presence metal oxide: Comparison of bromine fixation ability, *J Anal Appl Pyrol*, 91
412 (2011) 303-309.
- 413 [16] O. Terakado, R. Ohhashi, M. Hirasawa, Bromine fixation by metal oxide in pyrolysis of
414 printed circuit board containing brominated flame retardant, *J Anal Appl Pyrol*, 103 (2013) 216-
415 221.
- 416 [17] S. Oleszek, M. Grabda, E. Shibata, T. Nakamura, Fate of lead oxide during thermal treatment
417 with tetrabromobisphenol A, *J. Hazard. Mater.*, 261 (2013) 163-171.
- 418 [18] M. Rzyman, M. Grabda, S. Oleszek-Kudlak, E. Shibata, T. Nakamura, Studies on bromination
419 and evaporation of antimony oxide during thermal treatment of tetrabromobisphenol A (TBBPA),
420 *J Anal Appl Pyrol*, 88 (2010) 14-21.
- 421 [19] M. Altarawneh, B.Z. Dlugogorski, Mechanism of Thermal Decomposition of
422 Tetrabromobisphenol A (TBBA), *J. Phys. Chem. A*, 118 (2014) 9338-9346.
- 423 [20] G.-B. Liu, H.-Y. Zhao, T. Thiemann, Zn dust mediated reductive debromination of
424 tetrabromobisphenol A (TBBPA), *J. Hazard. Mater.*, 169 (2009) 1150-1153.
- 425 [21] EBFRIIP-European-Brominated-Flame-Retardant-Industry-Panel, TBBPA, in, 2009.
- 426 [22] D.Y. Lai, S. Kacew, W. Dekant, Tetrabromobisphenol A (TBBPA): Possible modes of action
427 of toxicity and carcinogenicity in rodents, *Food and Chemical Toxicology*, 80 (2015) 206-214.

- 428 [23] Q. He, X. Wang, P. Sun, Z. Wang, L. Wang, Acute and chronic toxicity of
429 tetrabromobisphenol A to three aquatic species under different pH conditions, *Aquatic Toxicology*,
430 164 (2015) 145-154.
- 431 [24] M. Grabda, S. Oleszek, E. Shibata, T. Nakamura, Vaporization of zinc during thermal
432 treatment of ZnO with tetrabromobisphenol A (TBBPA), *J. Hazard. Mater.*, 187 (2011) 473-479.
- 433 [25] S. Oleszek, M. Grabda, E. Shibata, T. Nakamura, Study of the reactions between
434 tetrabromobisphenol A and PbO and Fe₂O₃ in inert and oxidizing atmospheres by various thermal
435 methods, *Thermochim Acta*, 566 (2013) 218-225.
- 436 [26] M. Grabda, S. Oleszek, E. Shibata, T. Nakamura, Study on simultaneous recycling of EAF
437 dust and plastic waste containing TBBPA, *J. Hazard. Mater.*, 278 (2014) 25-33.
- 438 [27] S. Oleszek-Kudlak, M. Grabda, T. Nakamura, Alternative Method for Pyrometallurgical
439 Recycling of EAF Dust Using Plastic Waste Containing Tetrabromobisphenol A, *High
440 Temperature Materials and Processes*, 30 (2011) 359-366.
- 441 [28] M. Al-Harashsheh, S. Kingman, C. Somerfield, F. Ababneh, Microwave-assisted total
442 digestion of sulphide ores for multi-element analysis, *Anal Chem Acta*, 638 (2009) 101-105.
- 443 [29] M. Al-Harashsheh, S. Kingman, L. Al-Makhadmah, I.E. Hamilton, Microwave treatment of
444 electric arc furnace dust with PVC: Dielectric characterization and pyrolysis-leaching, *J. Hazard.
445 Mater.*, 274 (2014) 87-97.
- 446 [30] M. Al-Harashsheh, S. Kingman, A. Saeid, J. Robinson, G. Dimitrakis, H. Alnawafleh,
447 Dielectric properties of Jordanian oil shales, *Fuel Process Technol*, 90 (2009) 1259-1264.
- 448 [31] A.J. Cumbane, *Microwave Processing of Minerals*, in, University of Nottingham,
449 Nottingham, UK, 2003.
- 450 [32] M. Al-Harashsheh, A. Al-Otoom, L. Al-Makhadmah, I.E. Hamilton, S. Kingman, S. Al-Asheh,
451 M.A. Hararah, Pyrolysis of poly(vinyl chloride) and—electric arc furnacedust mixtures, *J. Hazard.
452 Mater.*, 299 (2015) 425-436.
- 453 [33] G.S. Lee, Y.J. Song, Recycling EAF dust by heat treatment with PVC, *Miner Eng*, 20 (2007)
454 739-746.
- 455 [34] M. Al-Harashsheh, M. Aljarrah, F. Rummanah, K. Abdellateef, S. Kingman, Leaching of
456 valuable metals from electric arc furnace dust - Tetrabromobisphenol A Pyrolysis residues, *J Anal
457 Appl Pyrol*, 125 (2017) 50-60.
- 458 [35] S. Oleszek, M. Grabda, E. Shibata, T. Nakamura, TG and TG-MS methods for studies of the
459 reaction between metal oxide and brominated flame retardant in various atmospheres,
460 *Thermochim Acta*, 527 (2012) 13-21.
- 461 [36] D.L. Perry, *Handbook of Inorganic Compounds*, 2nd ed., CRC Press, 2011.
- 462 [37] L.V. Gurvich, I.V. Veyts, C.B. Alcock, Thermodynamic properties of individual substances,
463 in: *Elements C, Si, Ge, Sn, Pb and thier compounds*, Hemisphere Publishing Corporation, New
464 York, 1991.
- 465 [38] T.A. Ioannidis, N. Kyriakis, A.I. Zouboulis, P. Akrivos, Lead and bromide precipitation from
466 aqueous acidic solutions. Potential exploitation in industrial applications, *Desalination*, 211 (2007)
467 272-285.

468

469

Research highlights

- Thermal and dielectric characteristics of EAFD, TBBPA and their mixtures were evaluated.
- EAFD-TBBPA mixtures absorbed microwaves effectively resulting in fast heating
- Selective separation of Zn and Pb leaving most iron in the solid residue was achieved

Microwave treatment of electric arc furnace dust with Tetrabromobisphenol A: Dielectric characterization and pyrolysis-leaching

Mohammad Al-harashsheh^{*1}, Sam Kingman², Ian Hamilton

¹ Chemical Engineering Department, Jordan University of Science and Technology, Irbid, 22110, Jordan

* msalharashsheh@just.edu.jo

²Faculty of Engineering, University of Nottingham, Nottingham, NG7-2RD, UK

Abstract

In the present work microwave treatment of electric arc furnace dust (EAFD) mixed with tetrabromobisphenol A (TBBPA) was investigated. A range of characterization techniques were used to understand the thermal behaviour of TBBPA-EAFD mixtures under microwave pyrolysis conditions. Dielectric and thermal properties of EAFD, TBBPA and their mixtures were determined. Both the dielectric constant and loss factor of the mixture were found to vary considerably with temperature and subsequently it was found that the mixtures of these materials absorbed microwaves effectively, especially at temperatures above 170⁰C. The high loss tangent of EAFD-TBBPA mixture above 170⁰C resulted in fast heating and high temperatures (above 700⁰C) resulting in reduction of Fe, Pb and Zn to their metallic form. This resulted in low recoveries of both Zn and Pb when the residue was leached in water. The recovery of Zn varied between 14 and 52 wt.%, while Pb recovery varied between 3 and 31 wt.% depending on microwave treatment efficiency. The low recovery of Zn and Pb could be ascribed by the reduction of metal oxides into their metallic form. More importantly this work has shown great selectivity in the leachability of both zinc and iron; with iron being left in the solid residue.

Keywords: EAFD; Dielectric Properties, Microwave treatment; Leaching; zinc extraction; TBBPA

1. Introduction

Electric Arc Furnace Dust (EAFD) is a waste by-product generated by the secondary steelmaking industry. Treatment of EAFD is of prime importance for environmental and resource conservation

27 as it is considered as an environmentally hazardous waste according to the Environmental
28 Protection Agency (EPA) as it contains easy leachable metals including Cd, Pb, and Cr [1, 2]. Due
29 to the depletion of the primary resources of metals such as Zn and Pb, recycling of this dust has
30 gained greater interest among researchers and investors in the metallurgical sector [3]. Both
31 Pyrometallurgical and hydrometallurgical methods have been suggested to recover valuable metals
32 from EAFD. Although pyrometallurgical treatment of EAFD is practiced now at the industrial
33 scale utilizing Waelz Kiln technology [4] and rotary hearth furnaces [5] to recover zinc in the form
34 of ZnO, these methods suffer from high energy requirements compared to hydrometallurgical
35 methods.

36 Different leaching reagents including sulphuric acid [6, 7], hydrochloric acid [8], ammonia [9, 10],
37 sodium hydroxide [11, 12], and some organic acids [13] have been used for extraction of zinc and
38 other valuables from EAFD. According to Jha et al [14], the most effective lixivants for zinc
39 extraction from EAFD were found to be sulphuric acid and ammoniacal solutions. Sodium
40 hydroxide dissolves zinc selectively, however, this application needs further development for
41 effective metal recovery from the sodium zincate solution by electrolysis.

42 There is a great interest nowadays to utilize waste halogenated plastic materials for the recovery
43 of valuable materials from EAFD and to minimize its environmental impact as well as that of waste
44 plastics. Among these waste plastic materials are flame retardant materials, with
45 tetrabromobisphenol A (TBBPA) being the most widely used. Thermal treatment of these wastes
46 results in release of large amounts of HBr and other brominated organic substances such as
47 brominated phenols as well as wide array of other brominated organic compounds [15-19]. If
48 TBBPA is pyrolysed in the presence of metal oxides, the later has high fixing ability toward HBr
49 and subsequent reduction of brominated organic compounds released during the pyrolysis process
50 [15, 20].

51 The largest volume brominated flame retardant in production today is TBBPA [21]; its annual
52 production exceeded 170 kilotons in 2004 [22] and the estimated annual market demand from 2001
53 to 2003 was >200,000 ton/year [23]. The reports suggest that huge quantities of brominated plastic
54 wastes are accumulated worldwide, which makes their disposal a real and current challenge.

55 Utilization of EAFD as a debromination catalyst for TBBPA based plastic materials offers
56 numerous benefits such as HBr capture liberated during TBBPA pyrolytic incineration in the form

57 of metal bromides. These can be recovered in their vapor form or leached from the pyrolysis
58 residue using just water. Such a technique allows two waste materials to be treated **concurrently**
59 to minimize their associated risks and at the same time recover valuable metals from EAFD by
60 relatively simple means.

61 A major decomposition product from TBBPA degradation is HBr; which is an excellent
62 brominating agent for ZnO present in EAFD and, it therefore, can be used as an agent to selectively
63 separate zinc as a volatile bromide from the solid dust residues. These properties lead to the use of
64 TBBPA as a source of (HBr) for zinc recovery from EAFD as zinc bromide $ZnBr_2$ [24, 25].

65 The de-bromination process is mainly the loss of bromination species from the backbone followed
66 by an evaporation process. Hydrogen **bromide** (HBr) as the brominating agent is generated in
67 relatively large amounts when the TBBPA decomposes during thermal processing (HBr accounts
68 for ca. 59 **wt.**% of TBBP upon thermal decomposition). The HBr reacts with zinc minerals forming
69 a bromide ($ZnBr_2$) that has a boiling point of 650°C. Grabda et al [24] studied the effect of heating
70 time and temperature on the vaporizing of $ZnBr_2$ under different conditions. They observed that
71 the evaporation increases with heating time at constant heating rate and increasing temperature
72 (due to an increase in the vapor pressure). A mixture of argon and oxygen were used to oxidize
73 the high molecular weight compound ('char') that formed during thermal decomposition of the
74 TBBPA and this affected the vaporization process; however this complex residue declined as
75 heating time and temperature increased. The measured vaporization data show that at 950° C the
76 vaporization of $ZnBr_2$ was complete, with less than 11 wt% char. However, one-third of ZnO
77 remained as un-reacted residue and required further treatment by carbothermic reduction by
78 carbonaceous char where 4 wt% remained in solid residue. Grabda et al. [26] continued to
79 investigate the possibility of EAFD treatment, using TBBPA and tetrabromobisphenol A
80 diglycidyl ether (TBBPADGE) at 550°C for 80 min, under oxidizing and inert atmospheres; a
81 maximum of 85**wt.**% of zinc and 81**wt.**% of lead recoveries were achieved using TBBPADGE.
82 Oleszek-Kudlak et al. [27] also studied the reaction **between** TBBPA **and** EAFD and the effect of
83 temperature on the of bromination **zinc oxide** and **the** evaporation of **its bromide ($ZnBr_2$) in the**
84 **temperature range 250 - 950 °C.**

85 This work aims at evaluating the possibility of heating EAFD-TBBPA mixtures by microwave
86 irradiation under pyrolysis conditions. It also aims to study the possibility of extracting valuable

87 metals from the pyrolysis residue by a hybrid microwave pyrolysis-extraction method. Therefore,
88 the dielectric properties of both materials (EAFD and TBBPA) and their mixtures were measured
89 using cavity perturbation technique and reported herein. Additionally, the pyrolysis of EAFD-
90 TBBPA mixtures, under microwaves, followed by leaching of microwave pyrolysis residue were
91 also carried out.

92 **2. Experimental work**

93 **2.1. Materials**

94 The EAFD sample was collected from a Jordanian steel smelter. After homogenization by repeated
95 cone and quartering, the sample was characterized for its chemical and mineralogical composition.
96 A **Perkin Elmer (Optima® 3300 DV)** Inductively Coupled Plasma Atomic Emission Spectrometer
97 (ICP-AES), was used to measure the content of elements in the EAFD following the procedure of
98 sample preparation reported by Al-**Harahsheh** et al [28]. TBBPA was purchased from Sigma
99 Aldrich. All other chemicals were reagent grade and used without further purification.

100 **2.2. Microwave treatment procedure**

101 The description of the experimental setup used for microwave treatment of the EAFD-TBBPA
102 mixtures is reported elsewhere [29]. It consisted of a 3 kW microwave generator operated at 2.45
103 GHz a forward and reflected power measurement system connected to a PC, a WR340 standard
104 rectangular waveguide operating in a dominate TE_{10} mode coupled to a cylindrical choke section
105 (for sampling). The reaction system consisted of nitrogen cylinder fitted with a **flow meter**, a
106 vertical quartz tube fitted inside the vertical applicator, two 250 ml gas wash bottles connected in
107 series and operated as gas extraction system, and vent connected to external extraction system.

108 EAFD was mixed with TBBPA in a tumbling mill with ceramic balls at a mass proportion of 1:1.
109 The mixture was then made into cylindrical pellets of about 5g mass. A hydraulic oil press was
110 then used to compress approximately 5 g of the mixture at 180 kg f/cm² for 60 s.

111 To perform the microwave pyrolysis experiments the pellets were placed in a quartz tube
112 positioned vertically in the cylindrical microwave applicator. The sample was then irradiated with

113 microwave energy for a specified time and power level while nitrogen gas purged the reaction
114 system. In order to collect any soluble vapors, the produced gases were vented through two gas
115 wash bottles filled with water. Irradiation time was varied depending on the observations of the
116 reaction systems **and also based on the temperature reading obtained by an optical pyrometer.**
117 Microwave power was shut-off if arcing occurred.

118 At the end of the experiment, the solid residues were reweighed and removed from the quartz tube.
119 Hot water was used to wash out the whole extraction system to collect any water soluble
120 condensate. It was then analyzed for metal content using ICP.

121 **2.3. Leaching of the microwave pyrolysis residues**

122 The solid residue after microwave treatment was ground to a particle size of less than 1 mm and
123 then subjected to leaching in boiling deionized water for 20 minutes. The mixture was then filtered
124 and the leaching solution was then analyzed for the metal content. The remaining solid residues
125 were also analyzed by X-ray diffraction (XRD) and Scanning Electron Microscopy (SEM).

126 **2.4. Measurement of dielectric properties**

127 Cavity perturbation method was employed to measure the dielectric properties of EAFD, TBBPA,
128 and their mixture. The experimental setup details are reported elsewhere [30]. A representative
129 mass of about 0.1-0.2 g of the material was packed in the quartz tube and heated to the desired
130 temperature, then positioned in the microwave resonant cavity by means of an automated actuator.
131 The frequency shift and quality factor were measured at 2470 and 912 MHz which are close to the
132 most frequently used frequencies in domestic and industrial microwave processes. Extra care was
133 taken to obtain similar packing density of samples, because powdered sample density has a great
134 effect on the measured values of dielectric properties [31]. The variation in density of packing for
135 3 replicates was determined to be less than 3.5%. Additionally for each sample, a minimum of
136 three replicates were measured. The dielectric constant (ϵ') and loss factor (ϵ'') were then calculated
137 [30].

138 **2.5.X-Ray diffraction and TGA analyses**

139 Representative EAFD sample, taken after prolonged manual mixing, was analyzed for its
140 mineral composition using X-ray diffraction analysis (XRD), furthermore, additional solid
141 samples were analyzed by XRD after microwave pyrolysis and after leaching experiments. A
142 Hiltonbrooks® generator with a Philips® PW 1050 diffractometer with an automatic divergence
143 slit, and Cu-K α anode producing X-rays of wavelength $\lambda= 1.54056 \text{ \AA}$ was used.

144 Thermogravimetric (TGA) and differential thermal analyses (DTA) of the dust (EAFD) and
145 the plastic material (TBBPA) and their mixture containing 50wt % EAFD and 50wt% TBBPA
146 were performed using a TA- Q600 thermal analyzer. About 10 mg of the sample was placed in
147 fused alumina pan and heated at a heating rate of 10°C/ min under nitrogen with a flow rate of 50
148 ml/min.

149 **3. Results and discussions**

150 **3.1.Physical and chemical characteristics of EAFD**

151 Figure 1 shows the XRD pattern of EAFD. The dust contains zincite, magnetite, franklinite,
152 halite, sylvite, lead hydroxyl chloride and hematite

153  Insert Figure 1

154 **Figure 1 XRD pattern for EAFD, EAFD-TBBPA residue after pyrolysis and after leaching**

155 The chemical composition of the EAFD sample used in this work was reported elsewhere
156 [32]. The main elements present in the dust are(in wt%) 25.9 Zn, 18 Fe, 4 Ca, 3.3 Na, 3.2 Pb, 2.8Si,
157 1.8 K and 1.2 Mn. Calorimetry showed that dust contains $2.63 \pm 0.03\text{wt}\%$ total carbon and 0.1wt%
158 inorganic carbon suggesting that among mineral phases present in the dust are carbonates such as
159 calcium carbonates.

160 **3.2. Dielectric properties of the EAFD**

161 The dielectric constant characterizes the capability of materials to absorb electromagnetic
162 radiation, whereas, loss factor denote the ability of materials to dissipate the adsorbed radiation

163 into heat. The dielectric constant and loss factor of EAFD were measured at two frequencies
164 namely 911 MHz and 2.47 GHz across a temperature range from 25 to 600 °C [29]. Figure 2 shows
165 the plot of dielectric constant (ϵ') and loss factor (ϵ'') as a function of temperature. Both values
166 increase with an increase of temperature and the rate of increase become greater when the
167 temperature exceeded 300 °C.

168 

169 **Figure 2 Dielectric properties of EAFD as a function of temperature) at frequencies of 911MHz and 2.47 GHz [4].**

170 Additionally, the ratio of dielectric loss to the dielectric constant is called loss tangent ($\tan \delta$).
171 When the loss tangent is above 0.05, the material is considered to heat well under microwave
172 irradiation. The loss tangent calculated for EAFD was found also to increase steadily with the
173 increase of temperature up to 300°C, then it increases considerably with a further increase of
174 temperature reaching a value of 0.3 at 600°C.

175 **3.3.Dielectric properties analysis of TBBPA**

176 **Figure 3** shows the dielectric properties of TBBPA as a function of temperature at frequencies of
177 911 and 2.47 GHz. The dielectric constant remains constant until a temperature of 150°C then
178 increases suddenly at a temperature of 170°C followed by steady increase until a temperature of
179 270°C and then decreases sharply. The loss factor decreases with the increase in temperature up
180 to a temperature of 150°C then increases sharply up to a temperature of 270°C and then drops
181 sharply. The increase of both dielectric constant and loss factor after 170°C is related to the start
182 of smelting of TBBPA (melting point of TBBPA=178°C). However the sharp decrease in both
183 parameters after 270°C is an artifact related to the sharp reduction of sample volume due to the
184 decomposition of TBBPA. To obtain more accurate dielectric properties values, a volume
185 correction factor should be introduced; the weight loss at the decomposition temperature was
186 measured to be around 75 wt% of the initial mass. **The data reported in Figure 5 did not take into**
187 **account the volume correction factor due to the difficulty in measuring the final volume at each**
188 **temperature.**

189 

190 **Figure 3 Dielectric Properties of TBBPA as a function of temperature at frequencies of 911 MHz and 2.47 GHz**

3.4. Thermal and dielectric properties of TBBPA-EAFD mixture

191
192 To study the interaction of the TBBPA-EAFD mixture with microwaves it is essential to measure
193 both dielectric constant and loss factor of the mixture. During thermal treatment of TBBPA-EAFD
194 mixture several events are expected to occur, which will influence the dielectric properties of the
195 mixture. Therefore, the change in mass loss, the heat flow, the dielectric constant and loss factor
196 were measured at different temperatures for a mixture containing 50 wt. % TBBPA and 50 wt. %
197 EAFD. The results of these measurements are plotted in **Figure 4 and Figure 5**.

198 The presence of EAFD with TBBPA altered the TGA decomposition profile of TBBPA. Two main
199 regions of mass loss can be seen in the TGA profile for the TBBPA-EAFD mixture, whereas, only
200 one mass loss was seen for pure TBBPA. The later corresponds to the decomposition of TBBPA
201 which ended at a temperature of 350°C; the corresponding mass loss was 75wt% of the initial
202 mass; the mass loss from EAFD alone at this temperature is only 2.5wt%. However, the mass loss
203 for TBBPA-EAFD at the first decomposition stage, ending at a temperature of 310°C, and was
204 21.5wt% although the decomposition event occurred at the same initial temperature. With the
205 mixture containing 50wt% TBBPA and the remainder consisting of EAFD; the expected mass loss
206 based on the losses of pure materials was determined to be 38.75wt% [29, 33]. The 17.25wt%
207 increase in residual mass found from the experiment is believed to be due to the HBr released not
208 leaving the sample, instead being fixed in the dust in the form of metal bromide (ZnBr_2 , PbBr_2 ,
209 CdBr_2 , FeBr_2 , FeBr_3 , etc). The exothermic event seen in the heat flow of the TBBPA-EAFD
210 mixture at a temperature of 310°C was evidence of the formation of metal bromides as seen in
211 **Figure 5**, whereas, an endothermic event was seen in the case of the pure TBBPA as a result of
212 decomposition.

213
214
215
216
217
218
219
220
221
222
223
224
225
226
227
228
229
230
231
232
233
234
235
236
237
238
239
240
241
242
243
244
245
246
247
248
249
250
251
252
253
254
255
256
257
258
259
260
261
262
263
264
265
266
267
268
269
270
271
272
273
274
275
276
277
278
279
280
281
282
283
284
285
286
287
288
289
290
291
292
293
294
295
296
297
298
299
300
301
302
303
304
305
306
307
308
309
310
311
312
313
314
315
316
317
318
319
320
321
322
323
324
325
326
327
328
329
330
331
332
333
334
335
336
337
338
339
340
341
342
343
344
345
346
347
348
349
350
351
352
353
354
355
356
357
358
359
360
361
362
363
364
365
366
367
368
369
370
371
372
373
374
375
376
377
378
379
380
381
382
383
384
385
386
387
388
389
390
391
392
393
394
395
396
397
398
399
400
401
402
403
404
405
406
407
408
409
410
411
412
413
414
415
416
417
418
419
420
421
422
423
424
425
426
427
428
429
430
431
432
433
434
435
436
437
438
439
440
441
442
443
444
445
446
447
448
449
450
451
452
453
454
455
456
457
458
459
460
461
462
463
464
465
466
467
468
469
470
471
472
473
474
475
476
477
478
479
480
481
482
483
484
485
486
487
488
489
490
491
492
493
494
495
496
497
498
499
500
501
502
503
504
505
506
507
508
509
510
511
512
513
514
515
516
517
518
519
520
521
522
523
524
525
526
527
528
529
530
531
532
533
534
535
536
537
538
539
540
541
542
543
544
545
546
547
548
549
550
551
552
553
554
555
556
557
558
559
560
561
562
563
564
565
566
567
568
569
570
571
572
573
574
575
576
577
578
579
580
581
582
583
584
585
586
587
588
589
590
591
592
593
594
595
596
597
598
599
600
601
602
603
604
605
606
607
608
609
610
611
612
613
614
615
616
617
618
619
620
621
622
623
624
625
626
627
628
629
630
631
632
633
634
635
636
637
638
639
640
641
642
643
644
645
646
647
648
649
650
651
652
653
654
655
656
657
658
659
660
661
662
663
664
665
666
667
668
669
670
671
672
673
674
675
676
677
678
679
680
681
682
683
684
685
686
687
688
689
690
691
692
693
694
695
696
697
698
699
700
701
702
703
704
705
706
707
708
709
710
711
712
713
714
715
716
717
718
719
720
721
722
723
724
725
726
727
728
729
730
731
732
733
734
735
736
737
738
739
740
741
742
743
744
745
746
747
748
749
750
751
752
753
754
755
756
757
758
759
760
761
762
763
764
765
766
767
768
769
770
771
772
773
774
775
776
777
778
779
780
781
782
783
784
785
786
787
788
789
790
791
792
793
794
795
796
797
798
799
800
801
802
803
804
805
806
807
808
809
810
811
812
813
814
815
816
817
818
819
820
821
822
823
824
825
826
827
828
829
830
831
832
833
834
835
836
837
838
839
840
841
842
843
844
845
846
847
848
849
850
851
852
853
854
855
856
857
858
859
860
861
862
863
864
865
866
867
868
869
870
871
872
873
874
875
876
877
878
879
880
881
882
883
884
885
886
887
888
889
890
891
892
893
894
895
896
897
898
899
900
901
902
903
904
905
906
907
908
909
910
911
912
913
914
915
916
917
918
919
920
921
922
923
924
925
926
927
928
929
930
931
932
933
934
935
936
937
938
939
940
941
942
943
944
945
946
947
948
949
950
951
952
953
954
955
956
957
958
959
960
961
962
963
964
965
966
967
968
969
970
971
972
973
974
975
976
977
978
979
980
981
982
983
984
985
986
987
988
989
990
991
992
993
994
995
996
997
998
999
1000

214 **Figure 4** overlay of mass loss and dielectric constant measurement (2.47 GHz) of 1:1 mass ratio of TBBPA-EAFD mixture
215 designated as E-TBBPA.

216 The second decomposition stage (470-600°C) seen in the TG profile of TBBPA-EAFD mixture
217 could be related to evaporation of zinc bromide formed [34]. Further mass loss occurring above
218 temperature 600°C could be related to evaporation of other metal bromides species like PbBr_2 and
219 FeBr_2 as well as reduction of the remaining metal oxides present in the dust by the char/carbon

220 (evidence of this will be demonstrated later) and also evaporation of metallic zinc produced by
221 reduction reactions.

222 The dielectric constant of the mixture did not correlate with the mass loss occurring at the first
223 decomposition stage as it increases with the increase in temperature up to a temperature of 550°C
224 reaching the first maxima of 13.2. The different behavior of dielectric constant of TBBPA-EAFD
225 mixture from that of pure TBBPA could be related to the formation ionic metal bromides which
226 coincide with TBBPA decomposition and the release of HBr. These halide ionic species exhibit
227 strong interaction with the electric field [29] due to ionic conduction and also the fusion of these
228 halides ($T_m(\text{ZnBr}_2)=394^\circ\text{C}$ [35]; $T_m(\text{PbBr}_2)=371^\circ\text{C}$) [36].

229 The steady drop in dielectric constant of the TBBPA-EAFD mixture beyond a temperature of
230 550°C until 760°C, reaching a minima of 11.16, could be related to the vaporization of the metal
231 bromides which corresponds to the second thermal event described above. Beyond a temperature
232 of 760°C, the dielectric constant starts to increase again reaching a second maxima (of 15.02) at a
233 temperature of 905°C. In this temperature region reduction of the remaining metal oxides occurs
234 by the char forming pure metal like Zn, Pb and Fe, as confirmed by SEM analysis shown below.
235 Furthermore, zinc boils at a temperature of 907 °C [35].

236 The loss factor of TBBPA-EAFD mixtures, remained at very low values until the TBBPA smelts
237 thereafter the values began to increase at a constant rate up to the decomposition temperature of
238 TBBPA. Further increases occurred with a higher rate until reaching a maximum value (3.46) at a
239 temperature of 480 °C, **which corresponds to** the onset temperature of the second thermal event
240 (zinc bromide vaporization). The loss factor then dropped to values as low as 0.68 at a temperature
241 of 630°C then remained almost constant until the temperature reached 780 °C, where it was seen
242 to increase rapidly. The loss of the ionic metal bromides beyond a temperature of 480 °C appeared
243 to have contributed to the drop in the loss factor, however, the formation of the char at pyrolysis
244 temperature is likely to the cause of the sharp increase of the loss factor.

245 **Insert Figure 5**

246 **Figure 5 overlay of heat flow and dielectric constant measurement (2.47 GHz) of 1:1 mass ratio of TBBPA-EAFD mixture**

247 3.5.Recovery of valuable metals

248 The recovery of valuable metals was performed for a TBBPA-EAFD mixture of mass ratio 1:1.
249 This was performed in two stages; metals evaporated during microwave pyrolysis and metals
250 leached from the pyrolysis residue using boiling water

251 The recovered metals from EAFD-TBBPA pellets after microwave pyrolysis in the extraction
252 system is shown in Table 1. The same experiment was repeated 6 times due to the great variations
253 in microwave coupling with the sample. Approximately 5wt% of zinc, 4wt% of lead and 6wt% of
254 cadmium were collected as metal bromide vapor. Other distinctive features observed (shown in
255 Table 1) was the absence of iron in the solution, implying that iron bromides were not evaporated
256 from the pellet.

257 **Table 1 Valuable metals (wt%) recovered as condensate in the extraction system after microwave treatment.**

Exp. #	Ca	Cd	Fe	K	Mg	Mn	Na	Pb	S	Zn
MH1	0.17	1.99	0.03	0.54	0.10	0.13	0.62	0.63	0.44	1.31
MH2	0.19	2.83	0.00	0.31	0.07	0.07	0.49	1.10	0.60	3.75
MH3	0.24	2.43	0.03	0.32	0.29	0.07	0.37	1.03	0.62	2.37
MH7	0.51	5.88	0.06	0.86	0.54	0.18	0.95	4.14	0.93	4.74
MH8	0.26	2.24	0.03	0.74	0.20	0.14	0.74	1.58	0.49	2.01
MH9	0.24	0.73	0.02	0.24	0.27	0.07	0.28	0.67	0.66	0.83

258 Table 2 shows the metal recovery from the TBBPA- dust mixtures after leaching of residues
259 obtained in hot water for 20 minutes. Both K and Na show high recovery in the leaching solution,
260 which is expected, as both K and Na are, initially, in the chloride form in the dust which are soluble
261 in water. Cadmium recovery was as high as 87wt% in the leaching solution, while the highest lead
262 and zinc recoveries were only 33wt% and 50wt%, respectively. **These values were slightly lower**
263 **than those obtained after conventional pyrolysis followed by leaching of the solid residues of E-**
264 **TBBPA1 (1 Dust: 1 TBBPA) [12].** With regards to iron, no more 1wt% was recovered in the
265 leaching solution and the remaining was mainly in the solid residue. This finding is of prime
266 importance, which suggests that excellent selectivity of dissolution of lead and zinc with respect
267 to iron, making further treatment of pregnant solution much simpler. **Similar selectivity results**
268 **were obtained under conventional pyrolysis conditions [33].** Additionally, both calcium and
269 manganese showed good fixing capacity toward HBr.

270

271 **Table 2 Valuable metals (wt%) recovered from TBBPA-EAFD mixtures by leaching of the pyrolysis residues in boiling**
 272 **water for 20 minutes**

Exp. #	Ca	Cd	Fe	K	Mg	Mn	Na	Pb	S	Zn
ML1	29.83	67.52	0.00	76.69	12.13	7.93	74.21	3.14	17.05	12.63
ML2	46.19	58.80	0.00	87.09	7.01	23.55	86.72	7.58	8.71	27.36
ML3	49.04	79.45	1.30	93.87	8.41	28.98	92.36	20.48	17.82	46.69
ML7	50.74	80.66	0.47	97.15	4.14	33.10	95.72	31.00	16.59	45.57
ML8	52.48	81.74	0.08	95.24	5.60	30.64	93.35	24.16	32.67	50.38
ML9	48.32	87.13	0.19	96.92	3.67	34.26	95.05	14.92	10.98	42.04

273 For a better understanding of the reaction occurring between metal oxides present in the dust and
 274 the decomposition products of TBBPA (HBr and char), both SEM and XRD analyses of both
 275 pyrolysis and leaching residues were performed.

276 The XRD patterns of solid residues after microwave pyrolysis, and after leaching with hot water
 277 are shown in Figure 1. Table 3 shows the main mineral phases identified in the samples (EAFD,
 278 pyrolysis and leaching residue). After pyrolysis the peaks of zincite decreased considerably,
 279 however, still present in the sample after pyrolysis and leaching which explains the low zinc
 280 recovery which is also related to the presence of franklinite. This could be due to several reasons
 281 the principal one being that the HBr released from the TBBPA was **stoichiometrically** not
 282 sufficient to convert all of ZnO and ZnFe₂O₄ to zinc bromide. It is worth mentioning that part of
 283 HBr was reacted with NaCl and KCl to form both NaBr and KBr.

284 The presence of chloride salts also led to the formation of complex salts such as Na₂ZnBr₄,
 285 Na₂PbBr₄, K₂ZnBr₄ and K₂PbBr₄. Additionally, the presence of wustite in the pyrolysis residue is
 286 an evidence of the partial iron oxide (magnetite) reduction.

287 SEM analysis of samples of the TBBPA-dust mixture after microwave treatment showed the
 288 formation of lead-iron nodules as can be seen from **Figure 6. These lead-iron nodules were not**
 289 **observed after conventional pyrolysis of the same mixture even at temperatures as high as 450 °C**
 290 . This suggests that the treatment temperature was high enough to carbonize the TBBPA and
 291 produce carbon that was able to reduce both iron and lead present in the dust. Such findings explain
 292 the lower recovery levels of iron, lead and zinc.

293 **Insert Figure 6**

294 **Figure 6 SEM micrograph and EDX analysis of TBBPA-dust residue (1:1) after microwave treatment showing iron nodules**
 295 **coated with lead.**

296 The XRD pattern for residue after leaching showed also the presence of Pb(OH)Br in the solid
297 residue, which explains the lower lead recovery than that of Zn. Ioannidis et al [37] reported that
298 Pb(OH)Br can be precipitated in neutral water in the pH range between 4-8. This was confirmed
299 by SEM and EDS analyses shown in Figure 7; the atomic ratio of Br and Pb is almost 1 suggesting
300 that the analyzed spot is Pb(OH)Br. The presence of Pb(OH)Br was also detected in the
301 conventional pyrolysis residue of the same mixture (50wt% EAFD+ 50wt% TBBPA) after
302 leaching [33]. Additionally, the atomic ratio of Fe, Zn and O is consistent with the presence of an
303 Fe-Zn alloy and iron and/or iron-zinc oxides; the atomic ratio of elements in franklinite is
304 1Zn:2Fe:4O, whereas, the ratio obtained in the area is 15Zn:19Fe:8O suggesting that almost
305 80wt% of Zn and Fe are in the form of Fe-Zn alloy. The latter was confirmed by XRD analysis
306 (see Table 3). However, such alloy was not detected in the previous work by Al-Harabsheh et al
307 [33] following conventional pyrolysis, which again confirms the high temperatures obtained by
308 microwave heating. The formation of char coupled with the high temperatures led to reduction of
309 Fe and Zn oxides into their metallic forms, while arcing during microwave pyrolysis have to their
310 smelting and formation of such Fe-Zn alloys.

311 In summary, it was found that microwave heating was efficient for the pyrolysis of TBBPA-EAFD
312 mixture in very short time (less than 2 minutes). An example of the power profile obtained during
313 microwave treatment of the mixture is shown in Figure 8. The amount of microwave power
314 absorbed increased rapidly reaching almost 80% of the incident power, and then dropped to almost
315 30%, followed by further increased to 60% after 1 minute then it remained constant. The absorbed
316 power profile is consistent with the variations in both dielectric constant and loss factor observed
317 shown in Figure 4 and Figure 5. . After 115 seconds of microwave arcing was observed, therefore,
318 the microwave power was shutoff. The maximum temperature detected by the optical pyrometer
319 was about 650 °C. However, for the purpose to recover metal values by leaching of pyrolysis
320 residue, it is required that the microwave pyrolysis temperature should not exceed 350°C to avoid
321 evaporation of metal bromides and the reduction of these metals into their metallic form.
322 Additionally, the ratio of TBBPA to EAFD should be increased to offer more HBr to convert both
323 zinc and lead oxides into soluble metal bromides. The recent work by Al-Harabsheh et al have
324 shown that conventional pyrolysis TBBPA-EAFD mixture up to a temperature of 350°C followed
325 by leaching of pyrolysis residue results in very high recoveries of both Zn and Pb leaving Fe in the
326 pyrolysis residue.

327 **Table 3 Mineral phases identified in the residue of EAFD-TBBPA (1:1) after microwave treatment and after water leaching.**

Feed EAFD	Franklinite/Magnetite, Zincite, Halite, Sylvite, PbCl(OH), calcite, silicate
EAFD-TBBPA residue after microwave pyrolysis	Franklinite/Magnetite, Zincite, PbBr ₂ , Willemite, Wustite, NaBr, KBr, K ₂ ZnBr ₄ , K ₂ PbBr ₄ , Na ₂ ZnBr ₄ , Na ₂ PbBr ₄ , Iron, Lead, Iron-zinc
EAFD-TBBPA residue after microwave pyrolysis and leaching	Franklinite/Magnetite, Zincite, Willemite, Wustite, Hematite, Iron, Lead, iron-zinc, PbBr(OH)

328

329

Insert Figure 7

330 **Figure 7 SEM micrograph and EDX analysis of TBBPA-dust residue (1:1) after microwave treatment and leaching showing**
 331 **PbBrOH precipitate**

332

Insert Figure 8

333 **Figure 8 Example of microwave power log obtained for Exp. MH 3**

334

335 **4. Conclusions**

336 Comprehensive characterization of EAFD-TBBPA mixture (ratio 1:1) was carried out in terms of
 337 their dielectric and thermal behavior as well as chemical and mineralogical composition. The
 338 TBBPA-EAFD mixture exhibited good absorption of microwaves once the melting temperature
 339 of the TBBPA has been reached. The microwave treatment time was short (1-3 minutes)
 340 suggesting the high efficiency of microwave treatment. Microwave treatment of EAFD-TBBPA
 341 mixture followed by water leaching was found to be not very efficient for recovery of Zn, and Pb
 342 due to the reduction of these metals into their metallic form by the carbonaceous materials left
 343 after TBBPA decomposition and also due to the low proportion TBBPA used in the mixture. The
 344 SEM and XRD analyses confirmed that part of iron, lead and zinc oxides present in the dust were
 345 reduced to their metallic form. Additionally Pb was found to precipitate during the leaching
 346 process in the form of PbBrOH which implies that Zn and Pb can be separated during leaching of
 347 the residue.

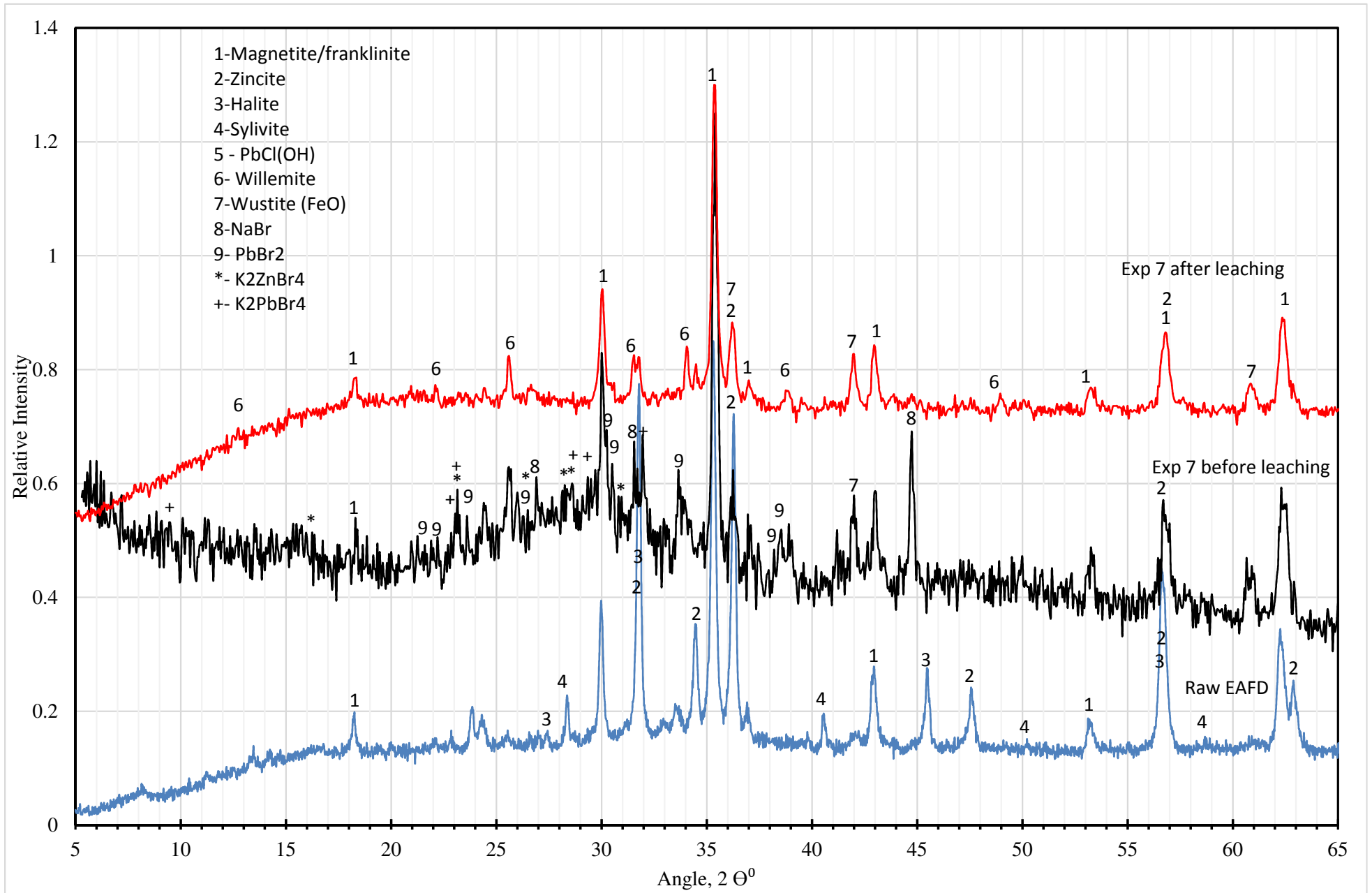
348 The pyrolysis of TBBPA in presence of EAFD is showed to be good method of debromination of
349 TBBPA to form a high value product. Although further work will be required to evaluate the
350 possibility of the emission of hazardous brominated organic compounds

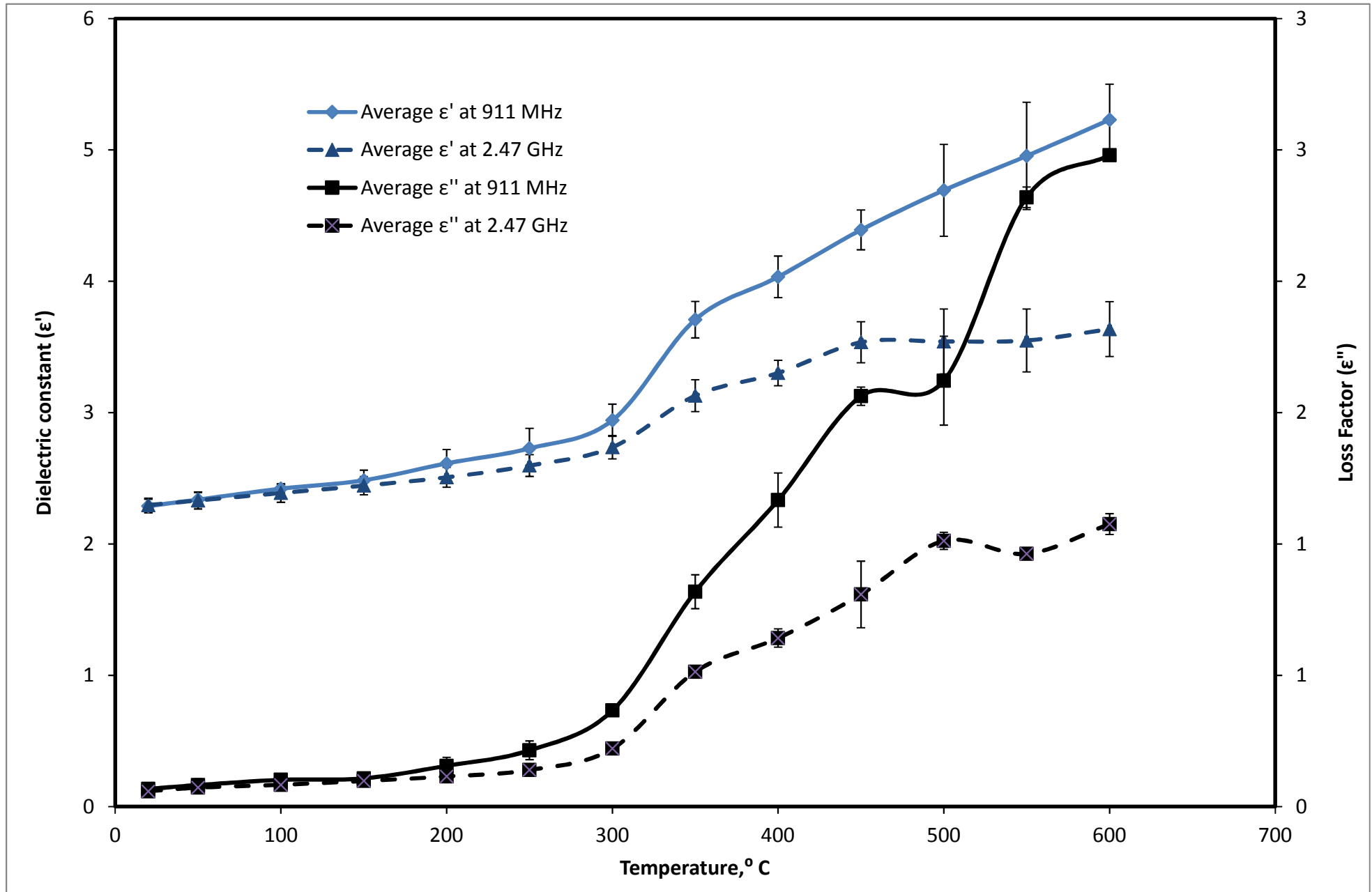
351 5. References

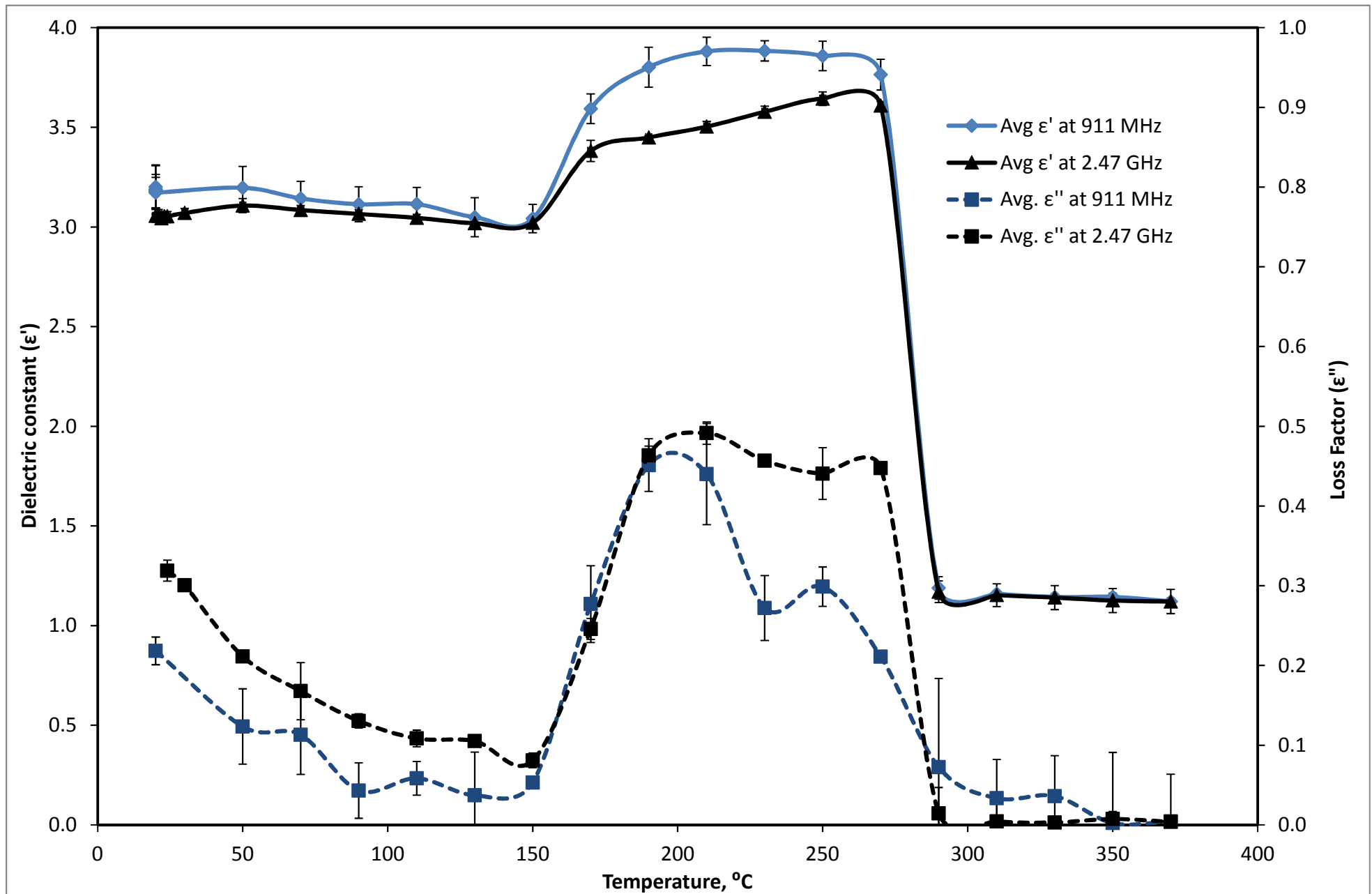
- 352 [1] T. Suetens, B. Klaasen, K. Van Acker, B. Blanpain, Comparison of electric arc furnace dust
353 treatment technologies using exergy efficiency, *Journal of Cleaner Production*, 65 (2014) 152-167.
- 354 [2] EAP, European Waste Catalogue And Hazardous Waste List in, Environmental Protection
355 Agency, 2002.
- 356 [3] E. Abkhoshk, E. Jorjani, M.S. Al-Harashsheh, F. Rashchi, M. Naazeri, Review of the
357 hydrometallurgical processing of non-sulfide zinc ores, *Hydrometallurgy*, 149 (2014) 153-167.
- 358 [4] J. Rütten, C. Frias, G. Diaz, D. Martin, F. Sanchez, Processing EAF dust through Waelz Kiln
359 and ZINCEXTM solvent extraction: the optimum solution, in: *European Metallurgical
360 Conference, SME, Düsseldorf/ Germany, 2011, pp. 1673-1688.*
- 361 [5] H. Oda, T. Ibaraki, Y. Abe, Dust recycling system by the rotary hearth furnace, in: *Nippon
362 Steel Technical Report, 2006, pp. 147-152.*
- 363 [6] T. Havlik, M. Turzakova, S. Stopic, B. Friedrich, Atmospheric leaching of EAF dust with
364 diluted sulphuric acid, *Hydrometallurgy*, 77 (2005) 41-50.
- 365 [7] F. Kukurugya, T. Vindt, T. Havlík, Behavior of zinc, iron and calcium from electric arc furnace
366 (EAF) dust in hydrometallurgical processing in sulfuric acid solutions: Thermodynamic and
367 kinetic aspects, *Hydrometallurgy*, 154 (2015) 20-32.
- 368 [8] D.S. Baik, D.J. Fray, Recovery of zinc from electric-arc furnace dust by leaching with aqueous
369 hydrochloric acid, plating of zinc and regeneration of electrolyte, *Mineral Processing and
370 Extractive Metallurgy*, 109 (2000) 121-128.
- 371 [9] Z. Youcai, R. Stanforth, Integrated hydrometallurgical process for production of zinc from
372 electric arc furnace dust in alkaline medium, *J. Hazard. Mater.*, 80 (2000) 223-240.
- 373 [10] K. Gargul, B. Boryczko, Removal of zinc from dusts and sludges from basic oxygen furnaces
374 in the process of ammoniacal leaching, *Archives of Civil and Mechanical Engineering*, 15 (2015)
375 179-187.
- 376 [11] A.J.B. Dutra, P.R.P. Paiva, L.M. Tavares, Alkaline leaching of zinc from electric arc furnace
377 steel dust, *Miner Eng*, 19 (2006) 478-485.
- 378 [12] C. Jarupisithorn, T. Pimtong, G. Lothongkum, Investigation of kinetics of zinc leaching from
379 electric arc furnace dust by sodium hydroxide, *Materials Chemistry and Physics*, 77 (2003) 531-
380 535.
- 381 [13] J.M. Steer, A.J. Griffiths, Investigation of carboxylic acids and non-aqueous solvents for the
382 selective leaching of zinc from blast furnace dust slurry, *Hydrometallurgy*, 140 (2013) 34-41.

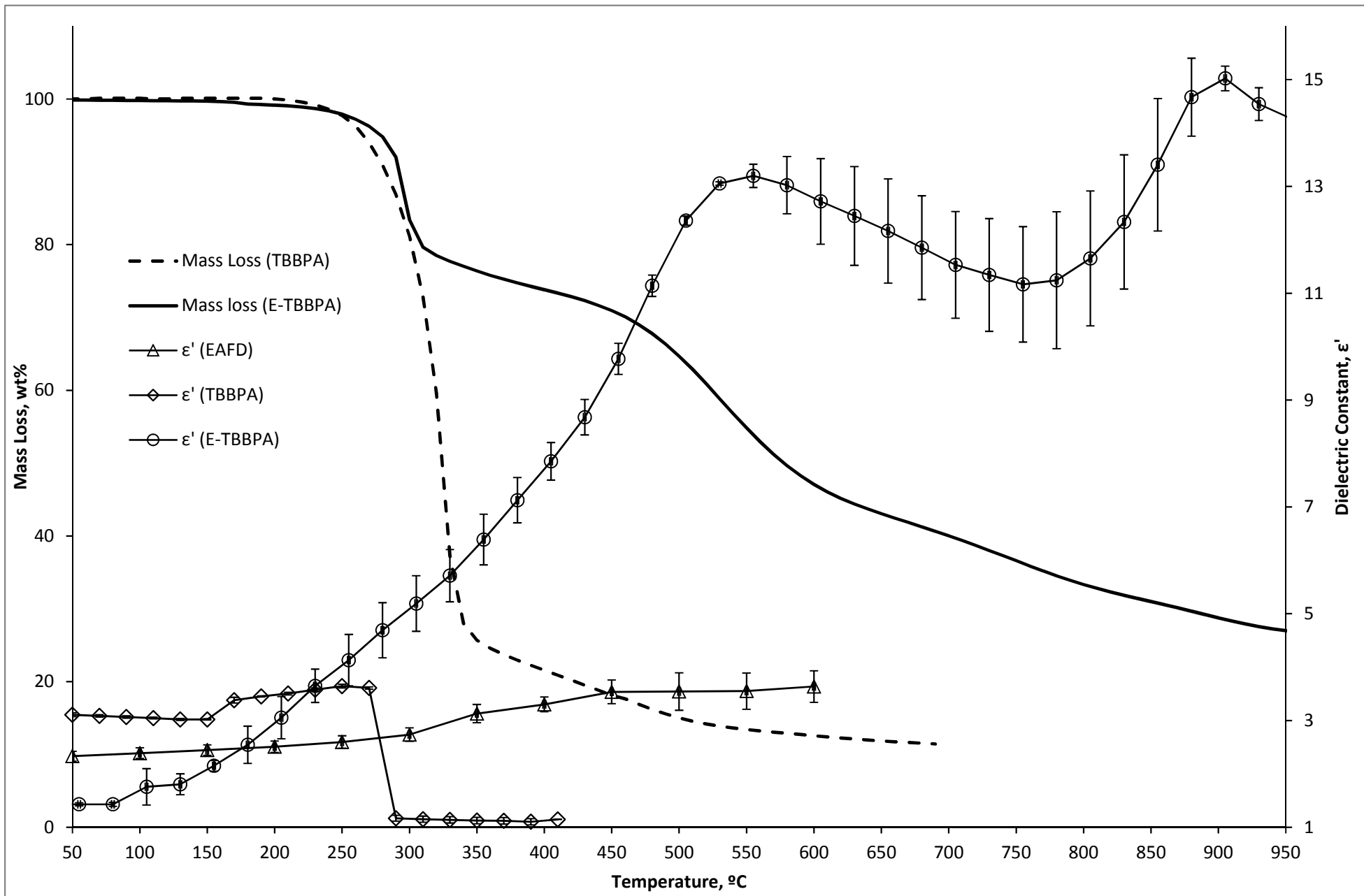
- 383 [14] M.K. Jha, V. Kumar, R.J. Singh, Review of hydrometallurgical recovery of zinc from
384 industrial wastes, *Resources, Conservation and Recycling*, 33 (2001) 1-22.
- 385 [15] O. Terakado, R. Ohhashi, M. Hirasawa, Thermal degradation study of tetrabromobisphenol
386 A under the presence metal oxide: Comparison of bromine fixation ability, *J Anal Appl Pyrol*, 91
387 (2011) 303-309.
- 388 [16] O. Terakado, R. Ohhashi, M. Hirasawa, Bromine fixation by metal oxide in pyrolysis of
389 printed circuit board containing brominated flame retardant, *J Anal Appl Pyrol*, 103 (2013) 216-
390 221.
- 391 [17] S. Oleszek, M. Grabda, E. Shibata, T. Nakamura, Fate of lead oxide during thermal treatment
392 with tetrabromobisphenol A, *J. Hazard. Mater.*, 261 (2013) 163-171.
- 393 [18] M. Rzyman, M. Grabda, S. Oleszek-Kudlak, E. Shibata, T. Nakamura, Studies on bromination
394 and evaporation of antimony oxide during thermal treatment of tetrabromobisphenol A (TBBPA),
395 *J Anal Appl Pyrol*, 88 (2010) 14-21.
- 396 [19] M. Altarawneh, B.Z. Dlugogorski, Mechanism of Thermal Decomposition of
397 Tetrabromobisphenol A (TBBA), *J. Phys. Chem. A*, 118 (2014) 9338-9346.
- 398 [20] G.-B. Liu, H.-Y. Zhao, T. Thiemann, Zn dust mediated reductive debromination of
399 tetrabromobisphenol A (TBBPA), *J. Hazard. Mater.*, 169 (2009) 1150-1153.
- 400 [21] EBFRI-P-Europian-Brominated-Flame-Retardant-Industry-Panel, TBBPA, in, 2009.
- 401 [22] D.Y. Lai, S. Kacew, W. Dekant, Tetrabromobisphenol A (TBBPA): Possible modes of action
402 of toxicity and carcinogenicity in rodents, *Food and Chemical Toxicology*, 80 (2015) 206-214.
- 403 [23] Q. He, X. Wang, P. Sun, Z. Wang, L. Wang, Acute and chronic toxicity of
404 tetrabromobisphenol A to three aquatic species under different pH conditions, *Aquatic Toxicology*,
405 164 (2015) 145-154.
- 406 [24] M. Grabda, S. Oleszek, E. Shibata, T. Nakamura, Vaporization of zinc during thermal
407 treatment of ZnO with tetrabromobisphenol A (TBBPA), *J. Hazard. Mater.*, 187 (2011) 473-479.
- 408 [25] S. Oleszek, M. Grabda, E. Shibata, T. Nakamura, Study of the reactions between
409 tetrabromobisphenol A and PbO and Fe₂O₃ in inert and oxidizing atmospheres by various thermal
410 methods, *Thermochim Acta*, 566 (2013) 218-225.
- 411 [26] M. Grabda, S. Oleszek, E. Shibata, T. Nakamura, Study on simultaneous recycling of EAF
412 dust and plastic waste containing TBBPA, *J. Hazard. Mater.*, 278 (2014) 25-33.
- 413 [27] S. Oleszek-Kudlak, M. Grabda, T. Nakamura, Alternative Method for Pyrometallurgical
414 Recycling of EAF Dust Using Plastic Waste Containing Tetrabromobisphenol A, *High*
415 *Temperature Materials and Processes*, 30 (2011) 359-366.
- 416 [28] M. Al-Harashsheh, S. Kingman, C. Somerfield, F. Ababneh, Microwave-assisted total
417 digestion of sulphide ores for multi-element analysis, *Anal Chem Acta*, 638 (2009) 101-105.
- 418 [29] M. Al-Harashsheh, S. Kingman, L. Al-Makhadmah, I.E. Hamilton, Microwave treatment of
419 electric arc furnace dust with PVC: Dielectric characterization and pyrolysis-leaching, *J. Hazard.*
420 *Mater.*, 274 (2014) 87-97.
- 421 [30] M. Al-Harashsheh, S. Kingman, A. Saeid, J. Robinson, G. Dimitrakakis, H. Alnawafleh,
422 Dielectric properties of Jordanian oil shales, *Fuel Process Technol*, 90 (2009) 1259-1264.

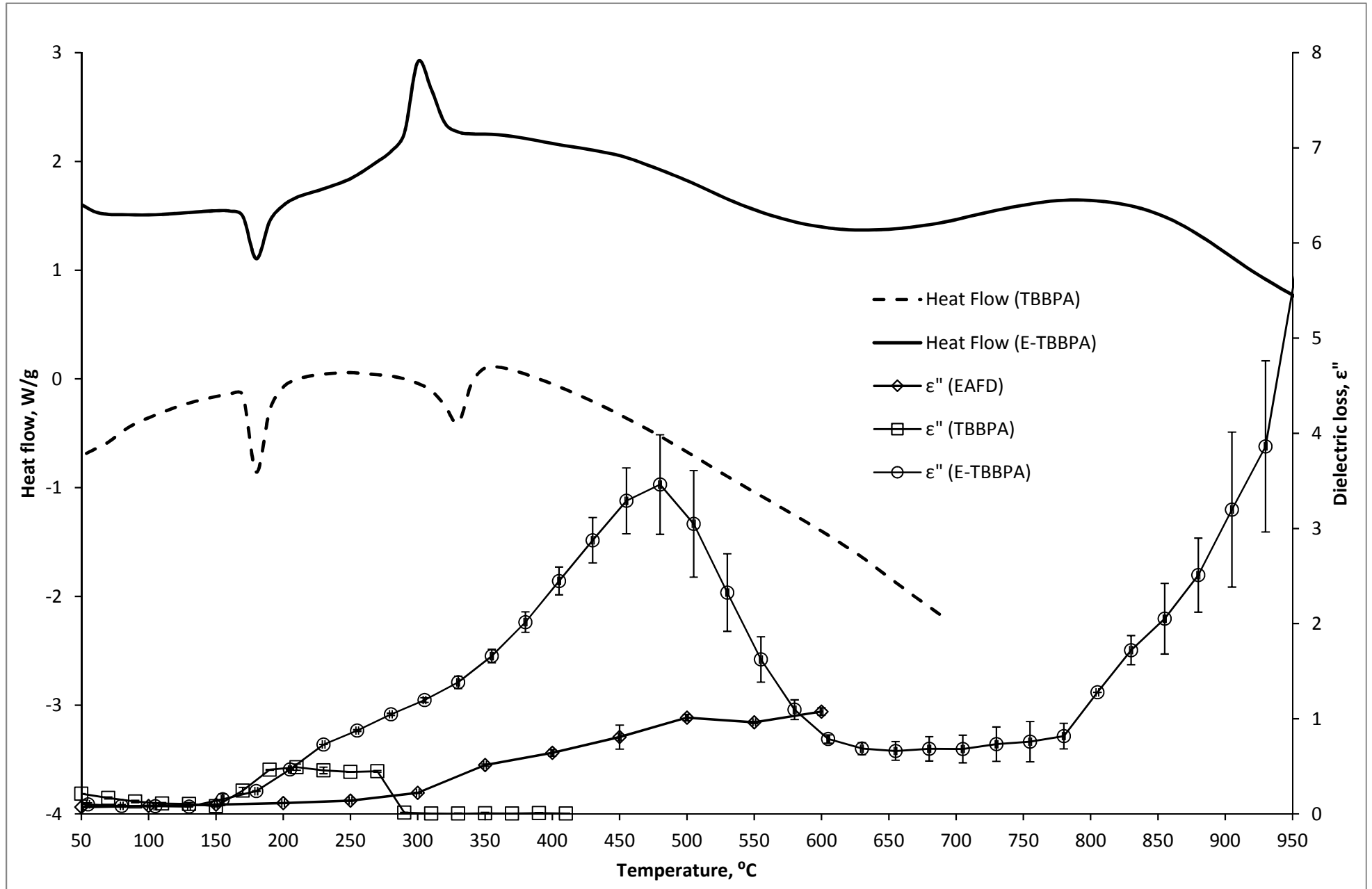
- 423 [31] A.J. Cumbane, Microwave Processing of Minerals, in, University of Nottingham,
424 Nottingham, UK, 2003.
- 425 [32] M. Al-Harashseh, A. Al-Otoom, L. Al-Makhadmah, I.E. Hamilton, S. Kingman, S. Al-Asheh,
426 M.A. Hararah, Pyrolysis of poly(vinyl chloride) and—electric arc furnacedust mixtures, J. Hazard.
427 Mater., 299 (2015) 425-436.
- 428 [33] M. Al-Harashseh, M. Aljarrah, F. Rummanah, K. Abdellateef, S. Kingman, Leaching of
429 valuable metals from electric arc furnace dust - Tetrabromobisphenol A Pyrolysis residues, J Anal
430 Appl Pyrol, 125 (2017) 50-60.
- 431 [34] S. Oleszek, M. Grabda, E. Shibata, T. Nakamura, TG and TG-MS methods for studies of the
432 reaction between metal oxide and brominated flame retardant in various atmospheres,
433 Thermochem Acta, 527 (2012) 13-21.
- 434 [35] D.L. Perry, Handbook of Inorganic Compounds, 2nd ed., CRC Press, 2011.
- 435 [36] L.V. Gurvich, I.V. Veyts, C.B. Alcock, Thermodynamic properties of individual substances,
436 in: Elements C, Si, Ge, Sn, Pb and thier compounds, Hemisphere Publishing Corporation, New
437 York, 1991.
- 438 [37] T.A. Ioannidis, N. Kyriakis, A.I. Zouboulis, P. Akrivos, Lead and bromide precipitation from
439 aqueous acidic solutions. Potential exploitation in industrial applications, Desalination, 211 (2007)
440 272-285.
- 441
- 442

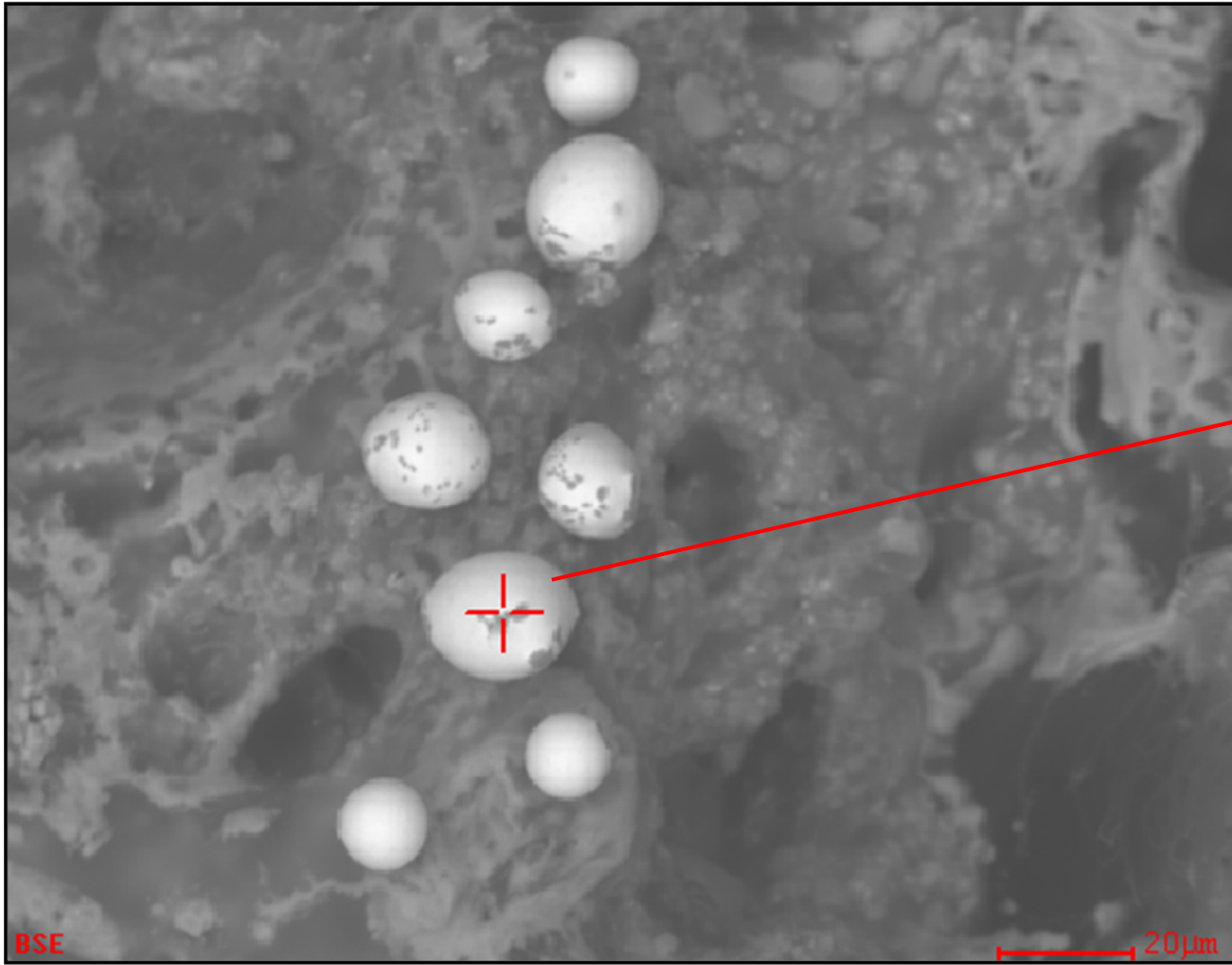




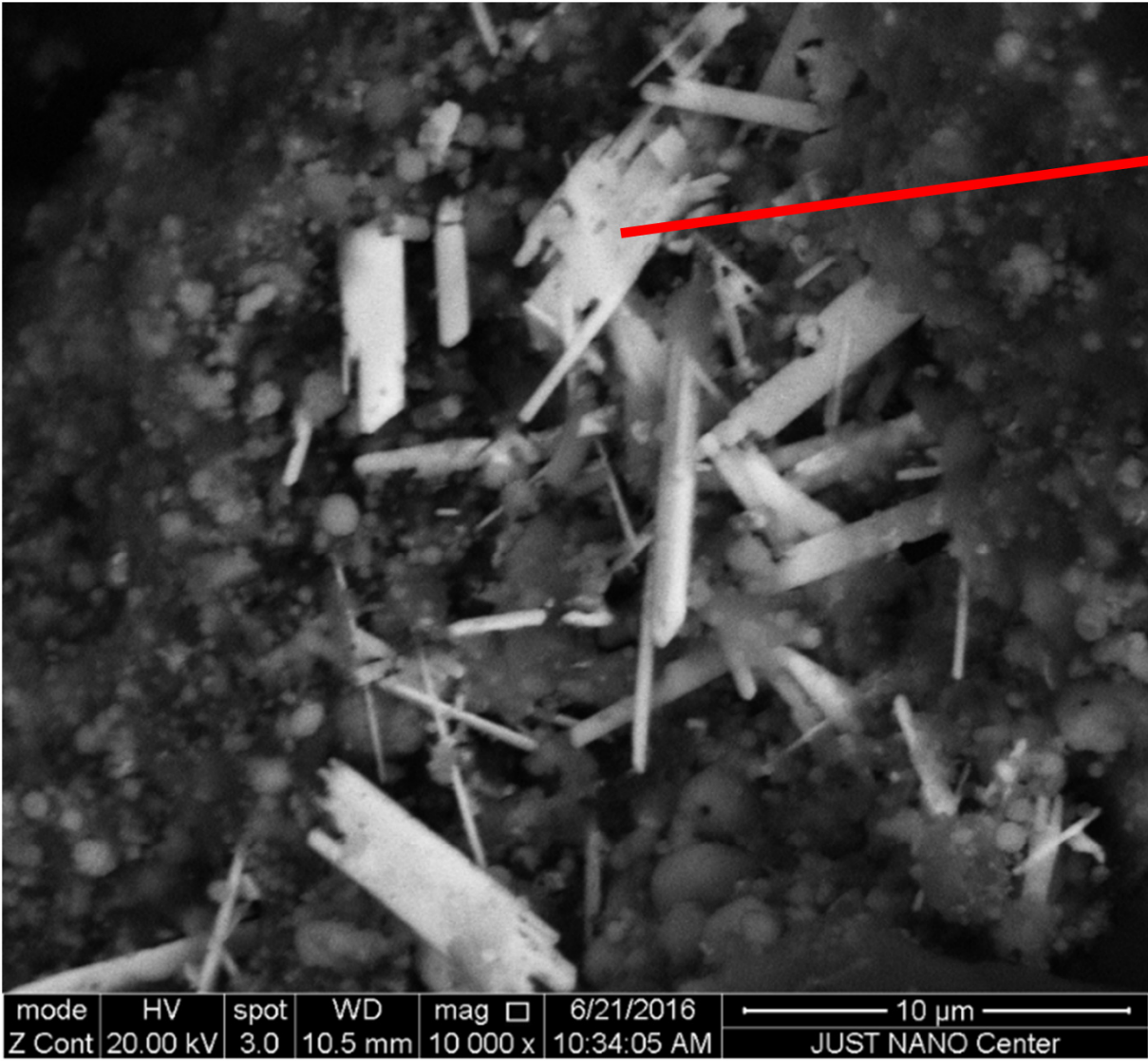




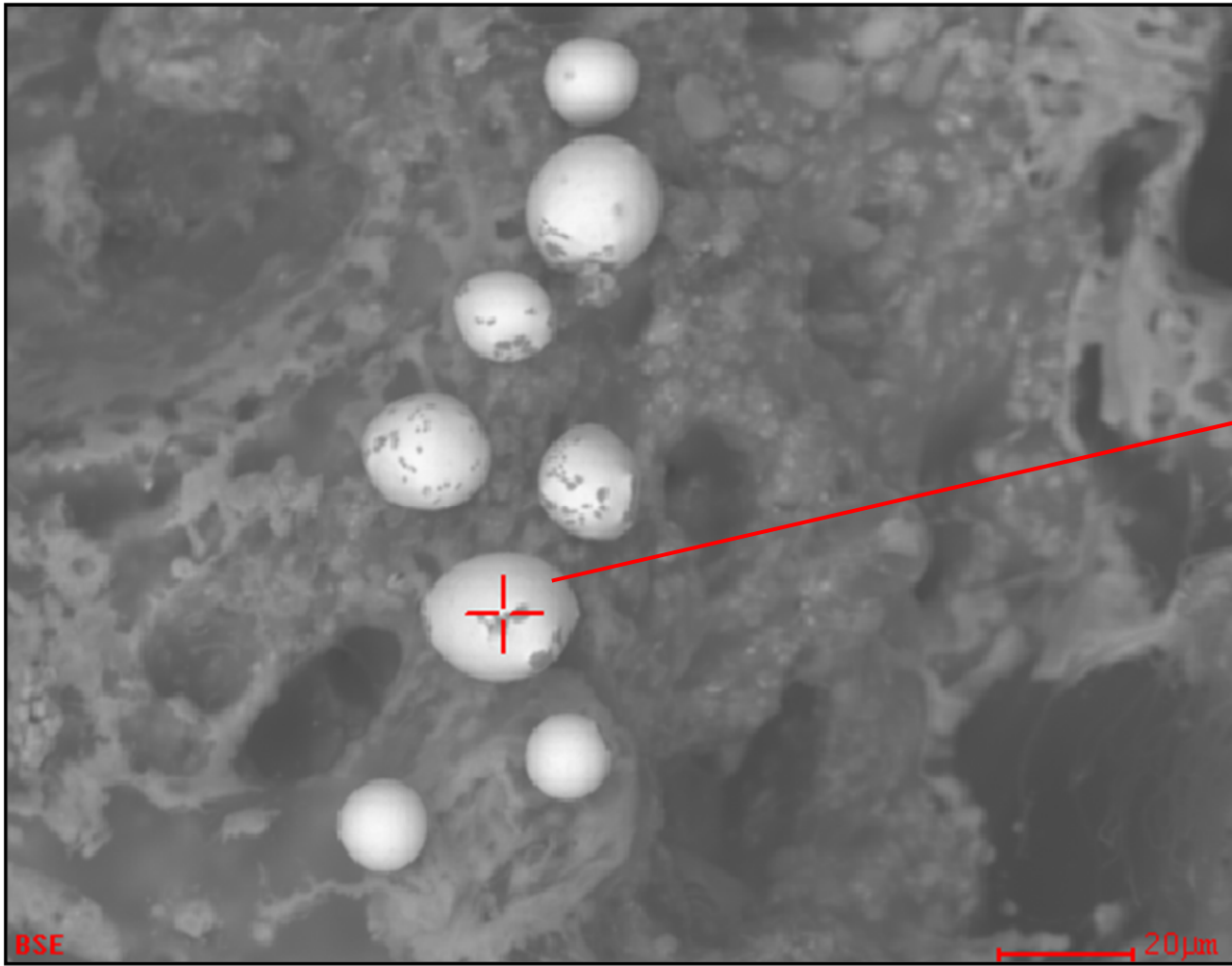




	<i>Wt%</i>	<i>At%</i>
<i>C_K</i>	15.79	55.17
<i>K_K</i>	0.40	0.43
<i>Ca_K</i>	0.44	0.46
<i>Fe_K</i>	42.65	32.05
<i>Zn_K</i>	2.62	1.69
<i>Pb_L</i>	30.38	6.15
<i>Br_K</i>	7.72	4.05



element	Wt %	%At
C _K	17.05	49.91
O _K	3.61	7.93
Al _K	1.5	1.95
Si _K	0.6	0.75
Ca _K	1.25	1.1
Fe _K	29.75	18.73
Zn _K	28.05	15.08
Pb _L	12.74	2.16
Br _K	5.35	2.35



	<i>Wt%</i>	<i>At%</i>
<i>C_K</i>	15.79	55.17
<i>K_K</i>	0.40	0.43
<i>Ca_K</i>	0.44	0.46
<i>Fe_K</i>	42.65	32.05
<i>Zn_K</i>	2.62	1.69
<i>Pb_L</i>	30.38	6.15
<i>Br_K</i>	7.72	4.05

